Cell

Sickle Hemoglobin Confers Tolerance to *Plasmodium* Infection

Ana Ferreira,[1] Ivo Marguti,[1] Ingo Bechmann,[2,3] Viktória Jeney,[1] Ângelo Chora,[1] Nuno R. Palha,[1] Sofia Rebelo,[1] Annie Henri,[4,5,6] Yves Beuzard,[4,5,6] and Miguel P. Soares[1,*]
[1]Instituto Gulbenkian de Ciência, 2780-156 Oeiras, Portugal
[2]Institute of Anatomy, University of Leipzig, Liebigstr. 13, 04103 Leipzig, Germany
[3]Dr. Senckenbergische Anatomie, Institute for Clinical Neuroanatomy, Johann Wolfgang Goethe-University, 60 -596 Frankfurt/Main, Germany
[4]Institut Universitaire d'Hematologie, Université Paris 7, France
[5]CEA, Institute of Emerging Diseases and Innovative Therapies, Fontenay-aux-Roses, France
[6]INSERM U962 and University Paris Sud 11, France
*Correspondence: mpsoares@igc.gulbenkian.pt
DOI 10.1016/j.cell.2011.03.049

SUMMARY

Sickle human hemoglobin (Hb) confers a survival advantage to individuals living in endemic areas of malaria, the disease caused by *Plasmodium* infection. As demonstrated hereby, mice expressing sickle Hb do not succumb to experimental cerebral malaria (ECM). This protective effect is exerted irrespectively of parasite load, revealing that sickle Hb confers host tolerance to *Plasmodium* infection. Sickle Hb induces the expression of heme oxygenase-1 (HO-1) in hematopoietic cells, via a mechanism involving the transcription factor NF-E2-related factor 2 (Nrf2). Carbon monoxide (CO), a byproduct of heme catabolism by HO-1, prevents further accumulation of circulating free heme after *Plasmodium* infection, suppressing the pathogenesis of ECM. Moreover, sickle Hb inhibits activation and/or expansion of pathogenic $CD8^+$ T cells recognizing antigens expressed by *Plasmodium*, an immunoregulatory effect that does not involve Nrf2 and/or HO-1. Our findings provide insight into molecular mechanisms via which sickle Hb confers host tolerance to severe forms of malaria.

INTRODUCTION

Several point mutations in the β-chain of human Hb, e.g. HbS ($^{\beta}$6Glu->Val) (Jallow et al., 2009; Williams et al., 2005b), HbC ($^{\beta}$6Glu->Lys)(Modiano et al., 2001) and HbE ($^{\beta}$26Glu->Lys)(Hutagalung et al., 1999), can confer a survival advantage to *Plasmodium* (*P.*) infection (Williams, 2006). When present in the homozygous form, some of these mutations, e.g. HbS, become pathologic causing hemolytic anemia, leading to accumulation of high levels of cell-free Hb and heme in plasma (Reiter et al., 2002). Individuals carrying the HbS mutation in the heterozygous form, i.e. the A/S sickle cell trait, also accumulate low (nonpathologic) levels of heme in plasma (Muller-Eberhard et al., 1968) and are protected against malaria (Allison, 1954; Beet, 1947; Jallow et al., 2009; Williams, 2006).

Once released from Hb, a phenomenon favored in the case of HbS (Hebbel et al., 1988), free heme becomes cytotoxic (Balla et al., 1992; Seixas et al., 2009; Gozzelino et al., 2010). This deleterious effect is countered by the expression of heme oxygenase-1 (HO-1, encoded by the *Hmox1* gene)(Balla et al., 1992; Ferreira et al., 2008; Gozzelino et al., 2010), a stress-responsive enzyme that catabolizes free heme into biliverdin, iron and carbon monoxide (CO)(Tenhunen et al., 1968). HO-1 expression is induced by free heme, through a mechanism that involves the ubiquitination-degradation of Kelch-like ECH-associated protein 1 (Keap1) (Kensler et al., 2007), a cytoplasmic repressor of the transcription factor NF-E2-related factor-2 (Nrf2)(Alam et al., 1999). Upon nuclear translocation, Nrf2 binds to the stress-responsive elements in the *Hmox1* promoter (Ogawa et al., 2001), a regulatory mechanism that plays a central role in the control of *Hmox1* expression in response to heme (Kensler et al., 2007).

HO-1 is protective against a wide variety of immune mediated inflammatory diseases (Nath et al., 1992; Soares and Bach, 2009) including experimental cerebral malaria (ECM)(Pamplona et al., 2007), a lethal neuroinflammatory syndrome that develops in *P. berghei* ANKA infected C57BL/6 mice and that mimics some of the pathologic features of human cerebral malaria (CM)(Mishra and Newton, 2009). This protective effect is mediated by CO, which binds cell-free Hb and inhibits its oxidation, thus preventing heme release from oxidized Hb (Hebbel et al., 1988) and hence the pathogenesis of ECM (Pamplona et al., 2007). Given that expression of HO-1 (Belcher et al., 2006; Jison et al., 2004) and production of CO (Sears et al., 2001) are induced in individuals carrying the HbS mutation we hypothesized that this might explain why individuals carrying the A/S sickle cell trait have a survival advantage against malaria (Allison, 1954; May et al., 2007; Williams et al., 2005b). We provide evidence demonstrating that this is the case.

RESULTS

Sickle Hb Confers a Survival Advantage against Malaria in Mice

Inoculation of C57BL/6 mice (Hb^{wt}) with *P. berghei* ANKA infected red blood cells (RBC) led within 6 to 12 days to the

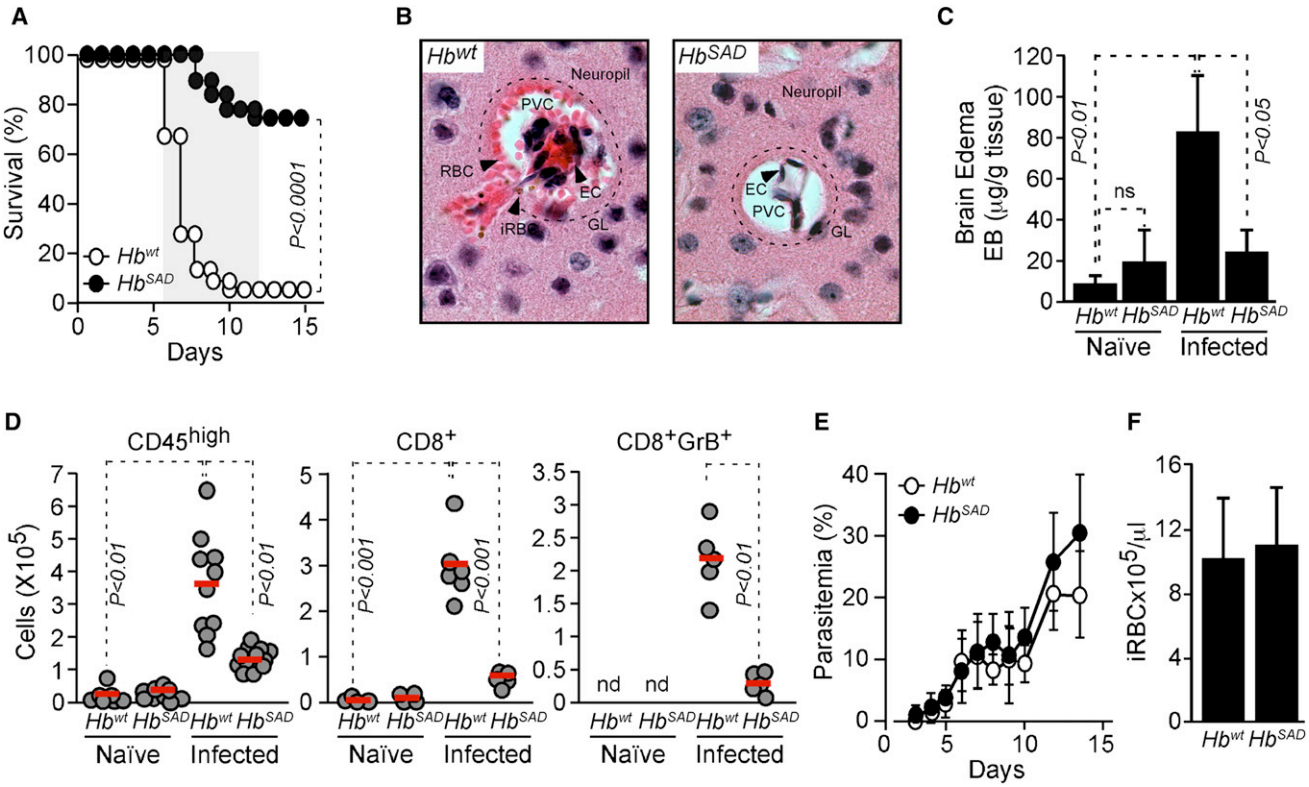

Figure 1. Hb^{SAD} Prevents ECM Onset

(A) Survival of *P. berghei* ANKA infected *Hb^{wt}* (n = 91) and *Hb^{SAD}* (n = 76) mice (10 independent experiments with survival advantage $p < 0.05$). Grey shading: expected time of ECM.

(B) Representative H&E stained microvessel in the BBB of infected *Hb^{wt}* and *Hb^{SAD}* mice, at ECM onset in *Hb^{wt}* mice (n = 3/group). EC: endothelial cell; PVC: perivascular compartment; GL: glia limitans (dotted line); RBC: red blood cells; iRBC: infected RBC. Magnification: 100x.

(C) Mean brain edema in naïve versus infected *Hb^{wt}* and *Hb^{SAD}* mice ± standard deviation (n=4/group), at the time of ECM onset in *Hb^{wt}* mice. ns: not significant.

(D) Brain leukocyte sequestration in naïve versus infected *Hb^{wt}* and *Hb^{SAD}* mice, at the time of ECM onset in *Hb^{wt}* mice. Dots represent single mice (n = 4 -14/group). Red lines represent mean values. nd: not determined.

(E) Mean percentage of infected RBC in *Hb^{wt}* and *Hb^{SAD}* mice ± standard deviation. Same mice as in (A).

(F) Mean number of infected RBC in *Hb^{wt}* (n=7) and *Hb^{SAD}* (n=9) mice ± standard deviation at the time of ECM onset in *Hb^{wt}* mice.

See also Figure S1 and Figure S2.

development of clinical signs of ECM (Figure 1A). Incidence of ECM was significantly reduced in hemizygous C57BL/6 *Hb^{SAD}* mice (Figure 1A) expressing a β-chain of human Hb carrying the $^{\beta}$6Glu->Val (Hb**S**) mutation as well as two additional mutations, $^{\beta}$23Ala->Ile (**A**ntilles^{23I}) and $^{\beta}$121Asp->Gln (D-Punjab^{121Q}), known to enhance HbS polymerization in humans and mice (Trudel et al., 1991). Naïve *Hb^{SAD}* mice present a very mild sickle cell syndrome, which does not lead to anemia (Table S1A available online; Trudel et al., 1994), similar to the asymptomatic human A/S sickle cell trait that affords protection against malaria (Allison, 1954; Beet, 1947; Jallow et al., 2009). *Hb^{SAD}* mice that did not develop ECM, succumbed 20-25 days postinfection from hyperparasitemia-induced anemia (data not shown), a condition unrelated to ECM (Schofield and Grau, 2005).

When infected with *P. berghei* ANKA, C57BL/6.Sv/129 *Hb$^{A/a}$* mice expressing normal human Hb as well as endogenous mouse Hb (Wu et al., 2006) developed clinical signs of ECM and succumbed 6 to 12 days after infection (Figure S1A). Littermate control C57BL/6.Sv/129 *Hb$^{a/a}$* mice, expressing only the endogenous mouse Hb developed ECM but with lower incidence, as compared to *Hb$^{A/a}$* mice (Figure S1A). This suggests that normal human Hb might promote, rather than prevent, the pathogenesis of ECM in C57BL/6.Sv/129 mice. While the reason for this is not clear, it is possible that human Hb alters mouse RBC physiology in a manner that would promote the development of ECM. However, this effect becomes negligible as C57BL/6.Sv/129 mice are backcrossed into the C57BL/6 genetic background (Figure S1D), in which ECM incidence is higher than 95% (Figure 1A). Given that *Hb^{SAD}* suppresses the pathogenesis of ECM in C57BL/6 mice and that the deleterious effect of normal human Hb becomes negligible under this genetic background, it is reasonable to infer that the protective effect of *Hb^{SAD}* is attributable to the mutations in the human β-globin chain rather than to human Hb *per se*.

Hb^{SAD} mice that did not succumb within 6–12 days postinfection also did not develop the pathologic hallmarks of ECM, including blood brain barrier (BBB) disruption (Figures 1B), perivascular RBC accumulation in brain (Figure 1B) and brain edema

(Figure 1C). These pathologic features were present in Hb^{wt} (Figures 1B and 1C) and $Hb^{A/a}$ mice, i.e. brain edema (Figure S1B).

Given that BBB disruption and brain edema occur in *P. berghei* ANKA infected C57BL/6 mice via a $CD8^+$ T cell-dependent mechanism (Belnoue et al., 2002; Schofield and Grau, 2005), we asked whether the protective effect of Hb^{SAD} against ECM was associated with inhibition of $CD8^+$ T cell sequestration in the brain. The number of $CD45^{high}$ leukocytes and $CD8^+$ T cells, including granzyme B-positive (GrB^+) $CD8^+$ T cells, was reduced in *P. berghei* ANKA infected Hb^{SAD}, as compared to Hb^{wt} mice at ECM onset (Figure 1D).

When infected with *P. berghei* ANKA, Hb^{wt} mice also developed severe lung injury and a mild form of liver injury (Figure S2) with no apparent injury to the kidneys or to the heart (*data not shown*). The extent of lung and liver injury was reduced in *P. berghei* ANKA infected Hb^{SAD} versus Hb^{wt} mice (Figure S2).

Sickle Hb Confers Tolerance to *Plasmodium* Infection in Mice

Protection of Hb^{SAD} mice against ECM was not associated with reduction of pathogen load, as assessed by the percentage of infected RBC, i.e., parasitemia (Figure 1E) as well as by the number of circulating infected RBC (Figure 1F) versus control Hb^{wt} (Figures 1E and 1F) or $Hb^{A/a}$ mice (Figures S1C and S1E). While the protective effect of the human sickle cell trait against malaria has been associated with decreased pathogen load (Allison, 1954; May et al., 2007; Williams et al., 2005b), there are several instances where this does not appear to be the case (Crompton et al., 2008; Livincstone, 1971; Motulsky et al., 1966), which is in keeping with the observation that Hb^{SAD} confers protection against ECM without interfering with pathogen load. These observations suggest that mutations in the β-chain of human Hb, such as those in Hb^{SAD} can afford tolerance to *Plasmodium* infection, a host defense strategy that limits disease severity by preventing tissue damage, without targeting the pathogen. This contrasts to resistance to infection, the well-recognized host defense strategy that limits disease severity by decreasing pathogen load (Raberg et al., 2007; Schneider and Ayres, 2008).

Parasite sequestration was similar in Hb^{wt}, $Hb^{SAD}Hmox1^{+/+}$, and $Hb^{SAD}Hmox1^{+/-}$ mice, as assessed using a transgenic luciferase-*P. berghei* ANKA strain (Figure 4S). This supports further the notion that induction of HO-1 by sickle Hb confers host tolerance to *Plasmodium* infection.

Sickle Hb Induces the Expression of HO-1 that Confers Tolerance to *Plasmodium* Infection

Humans and rodents carrying the HbS mutation express high levels of HO-1 in the hematopoietic compartment (Belcher et al., 2006; Jison et al., 2004). Consistent with this, naïve Hb^{SAD} mice express high levels of *Hmox1* mRNA in bone marrow and peripheral blood cells, as compared to naïve Hb^{wt} mice (Figure 2A). Naïve Hb^{SAD} mice also expressed higher levels of *Hmox1* mRNA in the kidneys (Figure S3A), which is consistent with the chronic development of kidney injury in these mice, revealed clinically upon aging (Sabaa et al., 2008). Hb^{SAD} mice expressed similar levels of *Hmox1* mRNA in the liver, heart, lung and spleen (Figure S3A), as compared to Hb^{wt} mice. $Hb^{A/a}$ mice expressed similar levels of *Hmox1* mRNA in the bone marrow and peripheral blood versus littermate control $Hb^{a/a}$ mice (*Suppl.* Figure 3B), demonstrating that expression of a β^S related variant but not a normal β-globin chain is required to induce *Hmox1* expression.

Given that HO-1 is protective against severe forms of malaria in mice (Pamplona et al., 2007; Seixas et al., 2009), we asked whether its induction in Hb^{SAD} mice (Figure 2A) is required to suppress the development of ECM (Figure 1A). Deletion of one *Hmox1* allele ($Hmox1^{+/-}$) reduced *Hmox1* mRNA expression in bone marrow and whole blood leukocytes of Hb^{SAD} mice (Figure S3C), without causing overt postnatal lethality (Table S2A). When challenged by *P. berghei* ANKA infection, $Hb^{SAD}Hmox1^{+/-}$ mice succumbed to ECM (Figure 2B), with concomitant development of BBB disruption (Figure 2C), brain edema (Figure 2D) and sequestration of $CD45^{high}$ leukocytes (*data not shown*), $CD8^+$ T cells and activated GrB^+CD8^+ T cells in the brain (Figure 2E) but without noticeable hematological changes (Table S1B).

The protective effect of Hb^{SAD} against lung and liver injury, associated with *P. berghei* ANKA infection, was lost in $Hb^{SAD}Hmox1^{+/-}$ mice (Figure S2). This was not associated with increased parasite load (Figure 2F).

Pharmacologic inhibition of HO activity by zinc protoporphyrin IX (ZnPPIX) (Figures S5A and S5B), increased ECM incidence in Hb^{SAD} mice versus vehicle-treated controls (Figure S5C). This effect was not associated with modulation of parasitemia (Figure S5D), suggesting that heme catabolism by HO-1 confers tolerance to *Plasmodium* infection in Hb^{SAD} mice.

Induction of HO-1 by Sickle Hb Inhibits the Production of Chemokines Involved in the Pathogenesis of ECM

Several chemokines can contribute to the pathogenesis of ECM and presumably to that of human CM (Campanella et al., 2008; Schofield and Grau, 2005; Mishra and Newton, 2009). Expression of mRNA encoding *Ccl2* (*Mcp-1*), *Ccl3* (*MIP1α*), *Ccl5* (*Rantes*), and *Cxcl10* (*Ip-10*) were decreased in the brain of Hb^{SAD} mice that did not develop ECM versus Hb^{wt} mice that succumbed to ECM (Figure 3A). This inhibitory effect involved HO-1, since expression of mRNA encoding these chemokines was increased in the brain of infected $Hb^{SAD}Hmox1^{+/-}$ versus $Hb^{SAD}Hmox1^{+/+}$ (Figure 3A). The involvement of CXCL10/IP-10 in the pathogenesis of ECM (Campanella et al., 2008) suggests that its inhibition might contribute functionally the protective effect of Hb^{SAD} against ECM. Expression of mRNAs encoding other chemokines, such as *Cxcl11* (*Ip-9*) or the chemokine receptors *Ccr2* and *Cxcr3* was also inhibited by Hb^{SAD} but in a manner that was not impaired in $Hb^{SAD}Hmox1^{+/-}$ versus $Hb^{SAD}Hmox1^{+/+}$ mice (Figure 3B). This suggests that the inhibitory effect of Hb^{SAD} over the expression of these genes, probably does not involve HO-1. Expression of mRNA encoding the chemokine *Ccl19* (*MIP-3β*) and the chemokine receptor *Ccr7* was not modulated by Hb^{SAD} and/or did not involve HO-1 (Figure 3C). This was also the case for several other genes previously involved or not in the pathogenesis of ECM (Figure S6 and Figure S7).

Sickle Hb Confers Tolerance to *Plasmodium* Infection via HO-1 Expression in Hematopoietic Cells

We performed syngenic bone marrow transplants from $Hb^{SAD}Hmox1^{+/+}$ or $Hb^{SAD}Hmox1^{+/-}$ mice into lethally irradiated

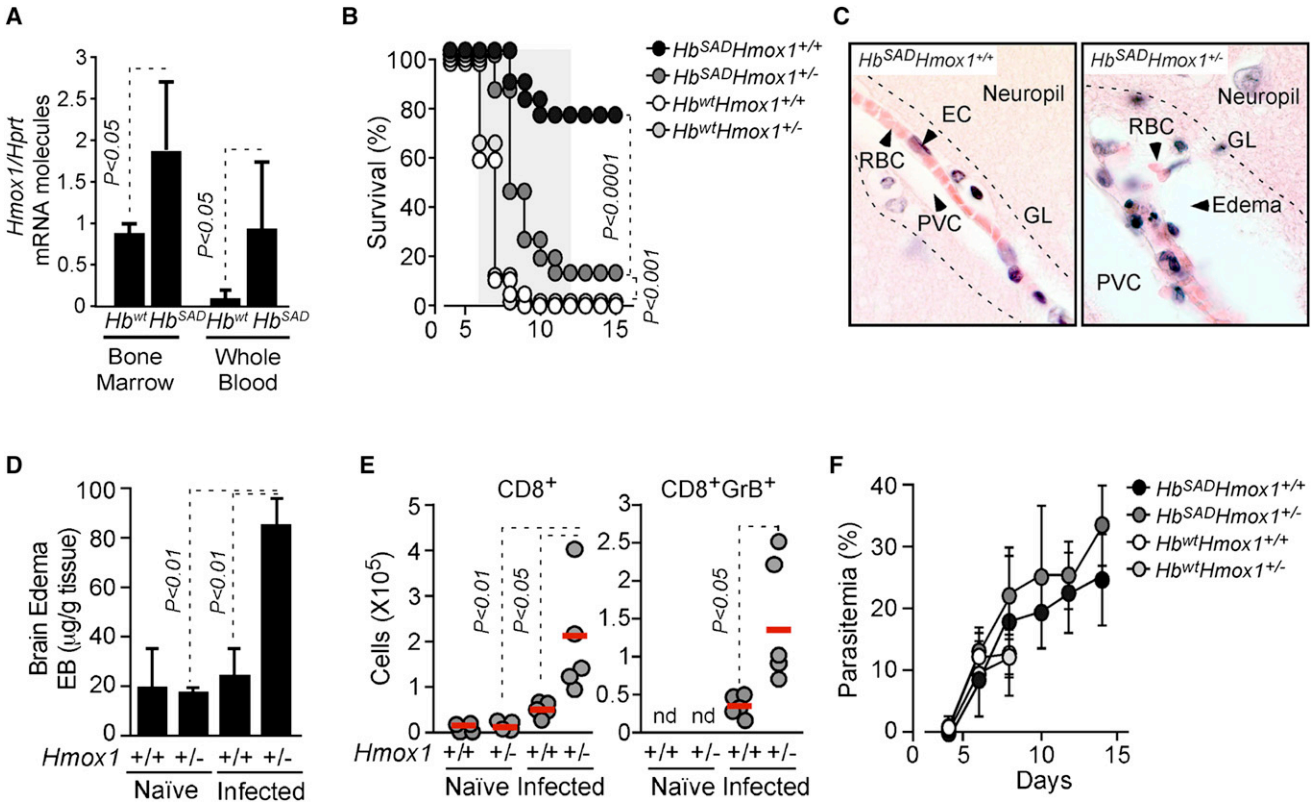

Figure 2. HO-1 Mediates the Protective Effect of Hb^{SAD} against ECM

(A) Mean ratio of *Hmox1* versus hypoxanthine-guanine phosphoribosyltransferase (*Hprt*) mRNA molecules in naïve Hb^{wt} and Hb^{SAD} mice ± standard deviation (n=4/group).

(B) Survival of *P. berghei* ANKA infected $Hb^{wt}Hmox1^{+/+}$ (n=19), $Hb^{SAD}Hmox1^{+/+}$ (n = 13), $Hb^{wt}Hmox1^{+/-}$ (n =15) and $Hb^{SAD}Hmox1^{+/-}$ (n = 15) mice. (three independent experiments; survival advantage $p < 0.05$). Grey shading: expected time of ECM.

(C) Representative H&E stained micro-vessel in the brain of infected $Hb^{SAD}Hmox1^{+/+}$ and $Hb^{SAD}Hmox1^{+/-}$ mice, at ECM onset in $Hb^{SAD}Hmox1^{+/-}$ mice (n=3/group). EC: endothelial cells; PVC: perivascular compartment; GL: glia limitans (dotted line); RBC: red blood cells. Magnification: 100×.

(D) Mean brain edema in naïve versus infected $Hb^{SAD}Hmox1^{+/+}$ and $Hb^{SAD}Hmox1^{+/-}$ mice, at ECM onset in $Hb^{SAD}Hmox1^{+/-}$ mice ± standard deviation (n = 3-4/group).

(E) $CD8^+$ T cells and activated GrB^+CD8^+ T cells in brains of naïve versus infected $Hb^{SAD}Hmox1^{+/+}$ and $Hb^{SAD}Hmox1^{+/-}$ mice, at the time of ECM onset in $Hb^{SAD}Hmox1^{+/-}$ mice. Dots represent single mice (n = 4–5/group). Red lines represent mean values. nd: not determined.

(F) Mean percentage of infected RBC (parasitemia) in the same mice as in (B). See also Figure S2, Figure S3, Figure S4, and Figure S5.

$Hb^{wt}Hmox1^{+/+}$ or $Hb^{wt}Hmox1^{+/-}$ mice to generate chimeric Hb^{SAD} mice in which one *Hmox1* allele is deleted in the hematopoietic ($Hb^{SAD}Hmox1^{+/-} \rightarrow Hb^{wt}Hmox1^{+/+}$) or nonhematopoietic ($Hb^{SAD}Hmox1^{+/+} \rightarrow Hb^{wt}Hmox1^{+/-}$) compartment. Chimeric Hb^{SAD} mice carrying two functional *Hmox1* alleles in the hematopoietic and in the nonhematopoietic compartments ($Hb^{SAD}Hmox1^{+/+} \rightarrow Hb^{wt}Hmox1^{+/+}$) did not succumb to ECM (Figure 4A) or develop brain edema (Figure 4B) in response to *P. berghei* ANKA infection. Control chimeric mice in which the bone marrow of $Hb^{wt}Hmox1^{+/+}$ mice was transferred into lethally irradiated $Hb^{SAD}Hmox1^{+/+}$ mice, develop ECM (Figure 4A) and brain edema (Figure 4B), confirming that cells derived from the hematopoietic compartment confer the protective effect of Hb^{SAD}.

Chimeric Hb^{SAD} mice carrying a single functional *Hmox1* allele in hematopoietic cells ($Hb^{SAD}Hmox1^{+/-} \rightarrow Hb^{wt}Hmox1^{+/+}$) succumbed to ECM (Figure 4A), developing brain edema (Figure 4B). The reverse was not true in that deletion of a single *Hmox1* allele in nonhematopoietic cells ($Hb^{SAD}Hmox1^{+/+} \rightarrow Hb^{wt}Hmox1^{+/-}$) did not impair the protective effect of Hb^{SAD} against ECM (Figure 4A), confirmed by lack of brain edema (Figure 4B). Similar results were obtained when transferring bone marrows from $Hb^{SAD}Hmox1^{+/+}$ or $Hb^{SAD}Hmox1^{+/-}$ mice into $Hb^{SAD}Hmox1^{+/+}$ or $Hb^{SAD}Hmox1^{+/-}$ mice Figure S8). Lethality after day 12 postinfection (Figure 4A) was most probably due to the development of a "composite disease" in which high levels of parasitemia (>20%) synergize with sickle human Hb to cause death, without overt clinical or pathological signs of ECM. These observations reveal that the protective effect of Hb^{SAD} requires the induction of HO-1 expression in hematopoietic cells, consistent with the observed induction of HO-1 expression in blood and bone marrow cells of naïve Hb^{SAD} mice (Figure 2A). The protective effect of HO-1 expression in the hematopoietic compartment was not associated with modulation of pathogen load (Figure 4C and Figure S8C), confirming that HO-1 affords tolerance to *Plasmodium* infection.

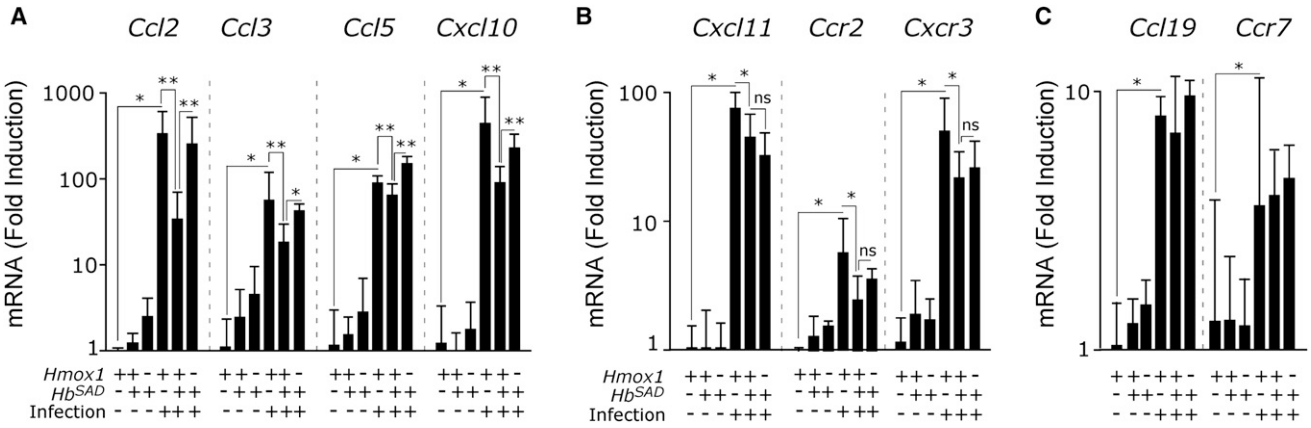

Figure 3. Induction of HO-1 by Hb^{SAD} Inhibits Chemokine Production in the Brain

Quantification of mRNA encoding chemokines and chemokine receptors in the brains of naïve (-) and *P. berghei* ANKA infected (+) mice carrying one (-) or two (+) functional *Hmox1* alleles and expressing (+) Hb^{SAD} or not (-). Results are shown as mean fold induction over naïve $Hb^{wt}Hmox1^{+/+}$ mice ± standard deviation (n = 4-8/group), analyzed at ECM onset in Hb^{wt} or $Hb^{SAD}Hmox1^{+/-}$ control groups.

(A) Genes inhibited by Hb^{SAD} under the control of HO-1.

(B) Genes inhibited by Hb^{SAD}, presumably not under the control of HO-1.

(C) Genes not regulated by Hb^{SAD}. *p < 0.05; **p < 0.01; ns P > 0.05. See also Figure S6 and Figure S7.

Sickle Hb Inhibits the Activation/Expansion of $CD8^+$ T Cells Recognizing Antigens Expressed by *Plasmodium*

The number of splenic $CD8^+$ T cells recognizing specifically a MHC I-restricted epitope derived from glycoprotein B ($gB_{498-505}$) of herpes simplex virus-1 expressed by transgenic *P. berghei* ANKA (Lundie et al., 2008) was reduced in Hb^{SAD} versus Hb^{wt} mice, as assessed five days after infection (Figure 4A *and* Figure S9A). The number of splenic GrB^+CD8^+ T cells was also reduced in Hb^{SAD} versus Hb^{wt} mice five days after infection (Figure 4E and Figure S9B). This reveals that Hb^{SAD} prevents overt expansion of pathogenic $CD8^+$ T cells, an effect that should contribute to the protective effect of Hb^{SAD} against ECM (Belnoue et al., 2002; Lundie et al., 2008). We then asked whether this immunoregulatory effect of Hb^{SAD} involved the expression of HO-1. The number of $gB_{498-505}$-specific $CD8^+$ T cells and GrB^+CD8^+ T cells was not different in the spleen of $Hb^{SAD}Hmox1^{+/-}$ versus $Hb^{SAD}Hmox1^{+/+}$ mice five days after infection (Figures 4D and 4E and Figures S9A and S9B). This suggests that Hb^{SAD} controls the activation and/or expansion of splenic $CD8^+$ T cells, via a mechanism that probably does not involve HO-1.

Sickle Hb Induces HO-1 Expression via a Mechanism Involving Nrf2

Given that Nrf2 plays a central role in the transcriptional regulation of HO-1 expression (Alam et al., 1999) we asked whether induction of HO-1 expression in whole blood leukocytes of naïve Hb^{SAD} mice (Figure 2A) involved this transcription factor. Deletion of one *Nrf2* allele in Hb^{SAD} mice ($Hb^{SAD}Nrf2^{+/-}$) was sufficient to reduce the level of *Hmox1* mRNA expression in whole blood leukocytes, to those of naïve $Hb^{wt}Nrf2^{+/+}$ mice (Figure 5A). This suggests that sickle Hb induces *Hmox1* transcription and expression via a mechanism involving Nrf2. Incidence of ECM increased significantly in *P. berghei* ANKA infected $Hb^{SAD}Nrf2^{+/-}$ versus $Hb^{SAD}Nrf2^{+/+}$ mice (Figure 5B), confirmed by the development of brain edema (Figure 5C). A similar effect was observed in a limited number of Hb^{SAD} mice in which both *Nrf2* alleles were functionally deleted, i.e. $Hb^{SAD}Nrf2^{-/-}$ mice (n = 5; 20% survival). It should be noted that deletion of both *Nrf2* alleles in Hb^{SAD} mice lead to overt postnatal lethality (Table S2B). Loss of protection against ECM in $Hb^{SAD}Nrf2^{+/-}$ versus $Hb^{SAD}Nrf2^{+/+}$ mice was not associated with a regain of $CD8^+$ T cell activation and/or expansion in the spleen, as assessed five days after infection (Figure S10). This suggests that the immunoregulatory of Hb^{SAD} probably does not involve Nrf2, which is consistent with the observation that this effect also does not seem to involve HO-1, a gene regulated by Hb^{SAD} via Nrf2 (Figure 5A).

The protective effect of Hb^{SAD} against lung and liver injury associated to *P. berghei* ANKA infection was lost in $Hb^{SAD}Nrf2^{+/-}$ versus $Hb^{SAD}Nrf2^{+/+}$ mice (Figure S2). This was not associated with increased parasite load in $Hb^{SAD}Nrf2^{+/-}$ versus $Hb^{SAD}Nrf2^{+/+}$ mice (Figure 5D), which is consistent with the notion that induction of HO-1 expression by Nrf2 confers tolerance to *Plasmodium* infection.

Sickle Hb Confers Tolerance to *Plasmodium* Infection via a Mechanism Involving CO Produced through Heme Catabolism by HO-1

Consistent with similar observations in individuals carrying the HbS mutation in the homozygous (Reiter et al., 2002) or heterozygous (Muller-Eberhard et al., 1968) form, naïve Hb^{SAD} mice had higher concentration of free heme in plasma, as compared to age-matched control naïve Hb^{wt} mice (Figure 6A). When pre-exposed in vitro to low levels of free heme cells are protected against a subsequent heme challenge (Balla et al., 1992). We asked whether free heme would exert a similar protective effect in vivo. Administration of free heme to Hb^{wt} mice prior to

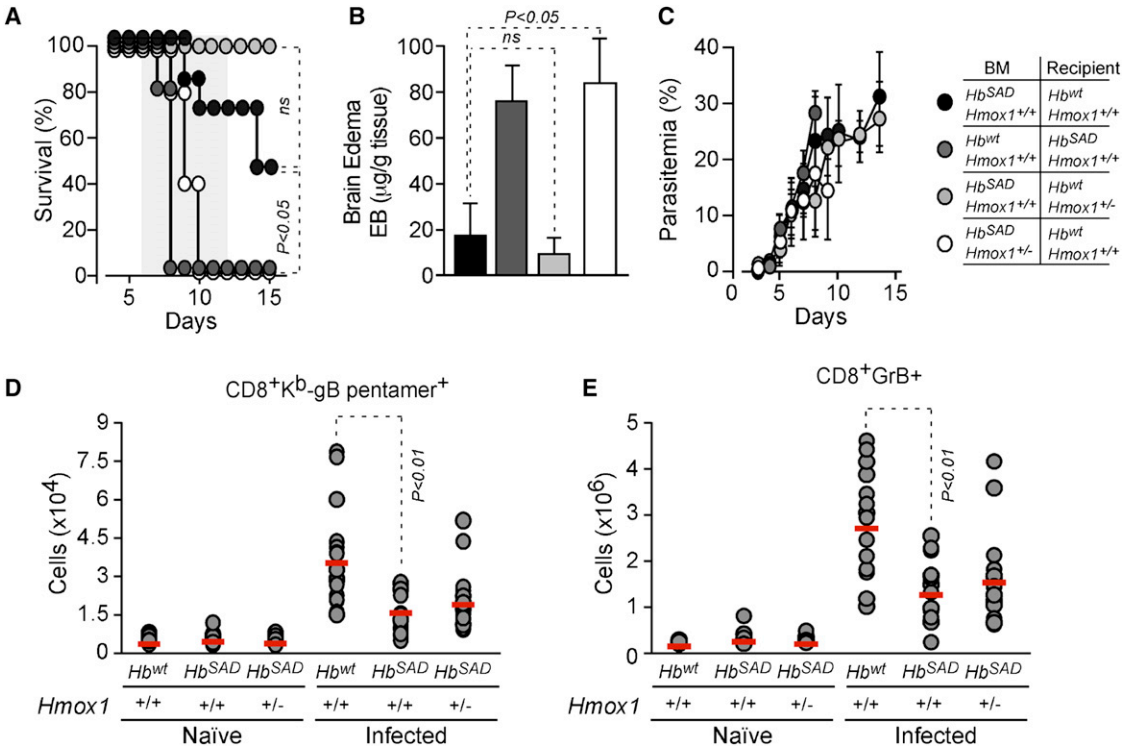

Figure 4. The Protective But Not The Immunoregulatory Effect of Sickle Hb against ECM Involves the Expression of HO-1 in Hematopoietic Cells

(A) Survival of *P. berghei* ANKA infected chimeric mice resulting from the adoptive transfer of bone marrow from $Hb^{SAD}Hmox1^{+/+}$ mice into $Hb^{wt}Hmox1^{+/+}$ recipients (n = 6); from Hb^{wt} $Hmox1^{+/+}$ mice into $Hb^{SAD}Hmox1^{+/+}$ recipients (n = 5); from $Hb^{SAD}Hmox1^{+/+}$ mice into $Hb^{wt}Hmox1^{+/-}$ recipients (n = 8) and from $Hb^{SAD}Hmox1^{+/-}$ into $Hb^{wt}Hmox1^{+/+}$ recipients (n = 7). Recipients were lethally irradiated before the adoptive transfer. Grey shading indicates expected time of ECM. Pooled from four independent experiments.

(B) Mean brain edema ± standard deviation (n = 3/group) in chimeric mice, produced as in (A).

(C) Mean percentage of infected RBC in chimeric mice ± standard deviation, same mice as in (A).

(D) Number of splenic $CD8^+$ T cells specific for $gB_{498\text{-}505}$ in $Hb^{wt}Hmox1^{+/+}$, $Hb^{SAD}Hmox1^{+/+}$ and $Hb^{SAD}Hmox1^{+/-}$ mice not infected (naïve) or 5 days after *P. berghei* ANKA infection.

(E) Number of splenic $CD8^+GrB^+$ T in the same mice as in (d). Circles in (d) and (e) represent single mice and red lines mean values (n = 10 and n = 16 in noninfected and infected groups, respectively), pooled from 4 independent experiments with similar results.

See also Figure S8 and Figure S9.

P. berghei ANKA infection suppressed ECM incidence, as compared to vehicle-treated Hb^{wt} mice (Figure 6B).

The protective effect of heme was dose-dependent, with higher dosage leading to (1) increased HO-1 expression in whole blood cells (Figure S1A) and spleen (Figure S1B) and to a lesser extent in the bone marrow (Figure S11C) and (2) suppression of ECM (Figure 11D). This protective effect was not associated with modulation of parasitemia (Figure S11D), suggesting that low concentration of free heme in the plasma of naïve Hb^{SAD} mice (Figure 6*a*) can confer tolerance to *Plasmodium* infection.

We asked whether accumulation of low levels of free heme in Hb^{SAD} contributes to the immunoregulatory effect exerted by Hb^{SAD} on $CD8^+$ T cells (Figures 4D and 4E). Administration of free heme to Hb^{wt} mice, prior to infection with transgenic *P. berghei* ANKA expressing $gB_{498\text{-}505}$, reduced the number of splenic $gB_{498\text{-}505}$-specific $CD8^+$ T cells (Figures S12A and S12B) as well as GrB^+CD8^+ T cells, as compared to vehicle treated Hb^{wt} mice five days after infection (Figures S12C and S12D). This supports further the notion that the protective effect of Hb^{SAD} against ECM is mediated, to a large extent, via the accumulation of low levels of circulating free heme.

Plasma free heme concentration increased significantly following *P. berghei* ANKA infection in Hb^{wt} mice (Figure 6A), an effect we have previously shown to contribute in a critical manner to the pathogenesis of ECM (Ferreira et al., 2008; Pamplona et al., 2007). Albeit less pronounced this increase was also observed in Hb^{SAD} mice (Figure 6A). When challenged with free heme after infection, Hb^{SAD} succumbed to ECM (Figure 6C), confirmed by the occurrence of brain edema (Figure 6*d*). This reveals that free heme has a dual effect in the control of ECM onset, being protective when present at slightly above normal concentration before infection (Figure 6B) while highly pathogenic when present at higher levels after infection (Figure 6C). Free heme did not interfere with pathogen load (Figures S11E and S11F), revealing that when present at slightly above normal concentration before infection free heme promotes tolerance to malaria, while impairing tolerance to malaria when present at

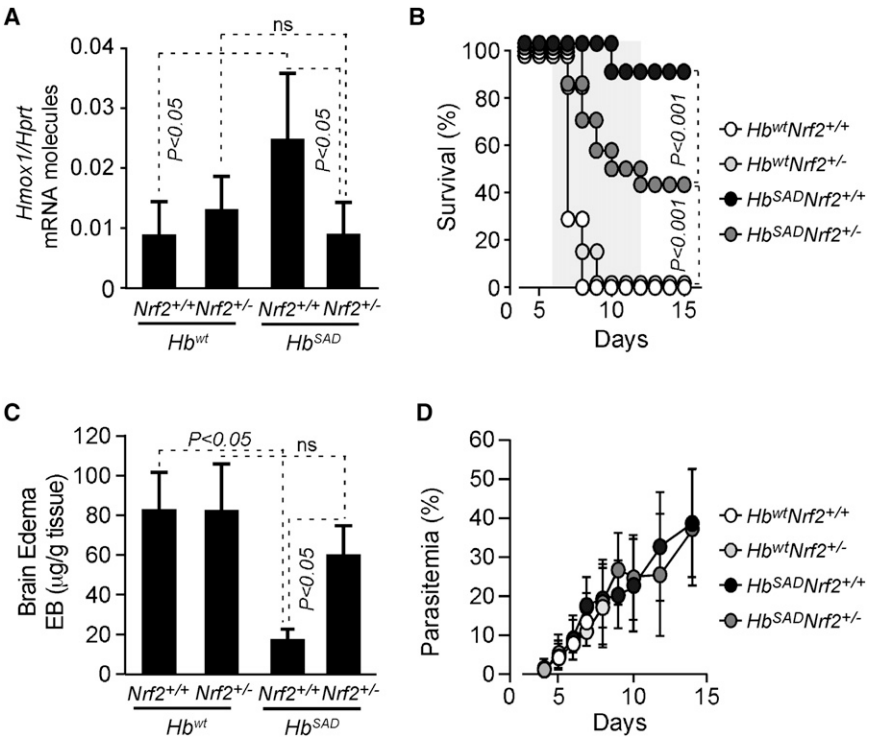

Figure 5. Sickle Human Hb Prevents the Onset of ECM via the Induction of HO-1 expression by Nrf2

(A) Mean ratio of *Hmox1* versus hypoxanthine-guanine phosphoribosyltransferase (*Hprt*) mRNA molecules in peripheral blood mononuclear cells of naïve $Hb^{wt}Nrf2^{+/+}$, $Hb^{wt}Nrf2^{+/-}$, $Hb^{SAD}Nrf2^{+/+}$ and $Hb^{SAD}Nrf2^{+/-}$ mice ± standard deviation (n = 6–8/group).

(B) Survival of *P. berghei* ANKA-infected $Hb^{wt}Nrf2^{+/+}$ (n = 6), $Hb^{wt}Nrf2^{+/-}$ (n = 13), $Hb^{SAD}Nrf2^{+/+}$ (n = 10) and $Hb^{SAD}Nrf2^{+/-}$ (n = 14) mice, three independent experiments. Grey shading indicates expected time of ECM.

(C) Brain edema was measured by Evans blue (EB) accumulation in brains of infected $Hb^{wt}Nrf2^{+/+}$, $Hb^{wt}Nrf2^{+/-}$, $Hb^{SAD}Nrf2^{+/+}$ and $Hb^{SAD}Nrf2^{+/-}$ mice, at the time of ECM onset. Mean ± standard deviation (n=4-5/group).

(D) Mean percentage of infected RBC (parasitemia) ± standard deviation, same mice as in (B). See also Figure S10.

higher concentrations after infection. Heme administration at the same dosage and schedule to naïve Hb^{wt} or Hb^{SAD} mice did not result in lethality (data not shown).

When applied via inhalation to wild type mice, CO suppresses the pathogenesis of ECM via a mechanism that relies on the inhibition of heme release from Hb (Pamplona et al., 2007). We asked whether the protective effect of Hb^{SAD} against ECM was mediated via this mechanism. Inhaled CO suppressed the incidence of ECM in $Hb^{SAD}Hmox1^{+/-}$ mice (Figure 6E), confirmed by the lack of brain edema (Figure 6F). A similar protective effect was observed when CO was applied to *P. berghei* infected Hb^{SAD} mice treated with the enzymatic HO inhibitor ZnPPIX (Figures S5E and S5F). CO did not modulate parasitemia (Figure 1G and Figures S11G and S11H). Instead, its protective effect was associated with reduction of plasma free heme concentration, below that of naïve $Hb^{SAD}Hmox1^{+/-}$ mice (Figure 6G). Administration of free heme to infected $Hb^{SAD}Hmox1^{+/-}$ mice abrogated the protective effect of CO, restoring ECM incidence (Figure 6H), confirmed by brain edema (Figure 6I). Heme was not toxic when administered at the same dosage and schedule to naïve $Hb^{SAD}Hmox1^{+/-}$ mice receiving CO, i.e. 0% mortality. These observations demonstrate that sickle Hb suppresses the onset of ECM via the induction of HO-1 and the production of CO, which inhibits the accumulation of free heme thus affording tolerance to *Plasmodium* infection (Figure 7).

DISCUSSION

The protective effect of sickle human Hb against malaria is thought to rely on the reduction of parasite load (Allison, 1954; May et al., 2007; Williams et al., 2005b), implying that sickle human Hb affords resistance (Raberg et al., 2007; Schneider and Ayres, 2008) to *Plasmodium* infection. Consistent with this notion, sickle human Hb decreases RBC permissiveness to *Plasmodium* invasion and growth (Friedman, 1978; Pasvol et al., 1978) while increasing phagocytosis of infected RBC, as assessed ex vivo (Ayi et al., 2004). Whether these effects account for the protective effect of sickle human Hb in vivo remained to be established. We used a well-established mouse model of malaria allowing for genetic manipulation of the host, to test in vivo the relative contribution of host specific genes to the protective effect of sickle Hb against *Plasmodium* infection. For technical and ethical reasons these studies can only be performed in rodent models of malaria.

As demonstrated hereby, sickle Hb affords protection against *Plasmodium* infection in mice (Figure 1A and Figure 2), a finding consistent with previous reports using different mouse and *Plasmodium* strains (Hood et al., 1996; Shear et al., 1993). This survival advantage occurs irrespectively of parasite load (Figures 1E and 1F) and is not associated with modulation of parasite sequestering in different organs (Figure S4), revealing that sickle human Hb confers tolerance (Raberg et al., 2007; Schneider and Ayres, 2008) to *Plasmodium* infection. This is consistent with our recent observation that heme catabolism by HO-1 also suppresses development of multiple organ dysfunction associated with the pathogenesis of severe sepsis in mice (Larsen et al., 2010), a lethal outcome of polymicrobial infection that resembles, in some aspects, severe malaria (Clark et al., 2004). Since the survival advantage conferred by HbS against malaria in human populations can occur without overt decrease of parasite load (Crompton et al., 2008; Livincstone, 1971; Motulsky et al., 1966), tolerance to *Plasmodium* infection might also operate in individuals expressing sickle Hb.

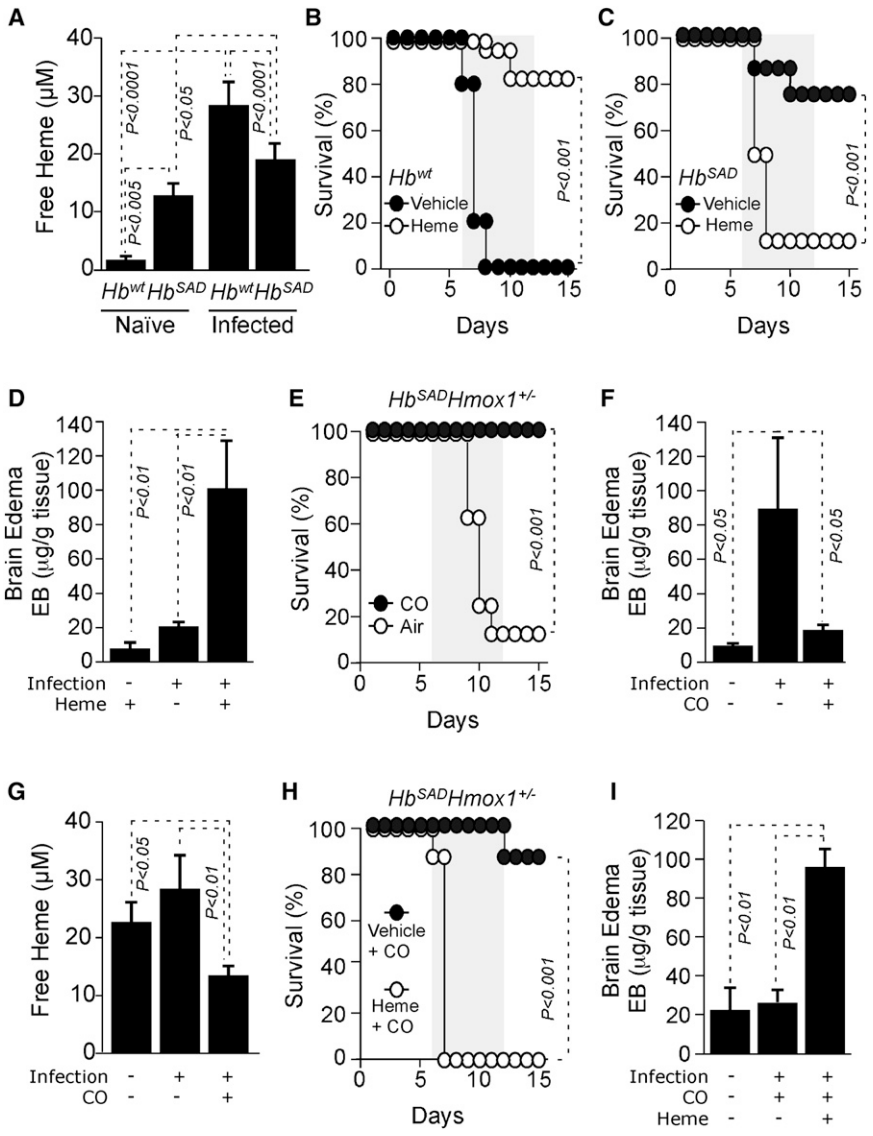

Figure 6. Hb^{SAD} Inhibits Free Heme Accumulation via the Production of CO

(A) Mean plasma free heme concentration in naïve versus *P. berghei* ANKA infected *Hb^{wt}* and *Hb^{SAD}* mice at ECM onset in *Hb^{wt}* mice ± standard deviation (n = 4–15/group).

(B) Survival of infected *Hb^{wt}* mice receiving vehicle (n = 25) or heme (35–40 mg/kg, every 48 hr, day 2 preinfection to 4 postinfection) (n = 17). Pooled from four independent experiments, with similar results.

(C) Survival of infected *Hb^{SAD}* mice receiving vehicle (n = 8) or heme (20 mg/kg, every 12 hr, day 4–7 postinfection) (n = 8). Pooled from two independent experiments, with similar results.

(D) Mean brain edema in *Hb^{SAD}* mice treated as in (c) at ECM onset in heme-treated *Hb^{SAD}* mice ± standard deviation (n = 4/group).

(E) Survival of infected *Hb^{SAD}Hmox1$^{+/-}$* mice exposed to air (n = 8) or CO (250 ppm, days 4-7 post infection) (n = 12). Pooled from three independent experiments, with similar results.

(F) Mean brain edema in *Hb^{SAD}Hmox1$^{+/-}$* mice treated as in (E), at ECM onset in air-treated mice ± standard deviation (n =3–4/group).

(G) Mean free heme in plasma of *Hb^{SAD}Hmox1$^{+/-}$* mice treated as in (E) ± standard deviation (n = 4–6/group).

(H) Survival of infected *Hb^{SAD}Hmox1$^{+/-}$* mice exposed to CO (250ppm; days 4–7 postinfection) and receiving vehicle (n = 8) or heme (20 mg/kg, every 12 hr, days 4–7 postinfection) (n = 8). Pooled from two independent experiments, with similar results.

(I) Mean brain edema in *Hb^{SAD}Hmox1$^{+/-}$* mice treated as in (H), at ECM onset in heme-treated mice ± standard deviation (n = 3–4/group). Grey shading in (B, C, E, and H) indicates expected time of ECM. See also Figure S11 and Figure S12.

We provide evidence for the existence of a specific molecular mechanism via which sickle human Hb confers tolerance to *Plasmodium* infection. When expressed at nonpathological levels in mice, sickle Hb leads to the accumulation of low concentrations of free heme in plasma (Figure 6A). The same is true for individuals carrying the sickle cell trait (Muller-Eberhard et al., 1968), which affords protection against malaria (Allison, 1954; Beet, 1947; Jallow et al., 2009; Williams, 2006). Presumably, this is due to the higher rate of heme release from sickle versus normal human Hb (Hebbel et al., 1988). In the absence of overt inflammation, free heme induces HO-1 expression without causing cytotoxicity (Balla et al., 1992; Gozzelino et al., 2010). Presumably, this explains how sickle human Hb induces the expression of HO-1 in human (Jison et al., 2004) and mouse (Figure 2A) peripheral blood mononuclear cells as well as in human endothelial cells (Bains et al., 2010; Nath et al., 2001). Expression of HO-1 prevents the cytotoxic effects of free heme (Balla et al., 1992; Gozzelino et al., 2010), hence limiting the pathological outcome of sickle cell anemia in mice (Belcher et al., 2006).

The mechanism via which sickle Hb induces the expression of HO-1 in vivo involves Nrf2 (Figure 5A), a transcription factor previously shown to regulate *Hmox1* expression (Alam et al., 1999; Kensler et al., 2007). Induction of HO-1 via Nrf2 affords protection against malaria in *Hb^{SAD}* mice expressing sickle Hb (Figure 2B and Figure 5B). This protective effect occurs irrespectively of parasite load (Figure 2F and Figure 5D) or parasite sequestration in different organs (Figure S4), revealing that sickle human Hb affords tolerance to *Plasmodium* infection via the Nrf2/HO-1 system.

The protective effect of HO-1 against sickle cell anemia (Belcher et al., 2006) and against malaria is mediated by the same end-product of heme catabolism, namely CO (Figures 6E and 6F). This gasotransmitter inhibits Hb oxidation and subsequently heme release from Hb (Hebbel et al., 1988) (Figure 6G), thus preventing free heme from participating in the pathogenesis

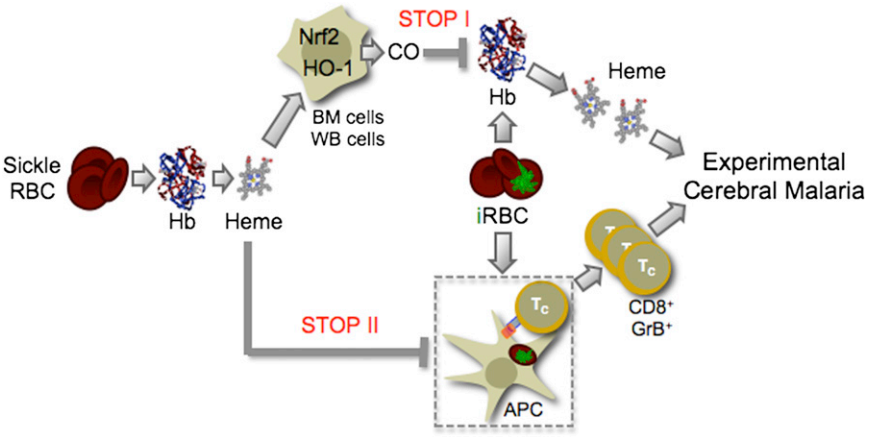

Figure 7. Protective Effect of Sickle Hb against ECM

Release of Hb from sickle RBC leads to chronic accumulation of cell-free Hb and release of its heme prosthetic groups. Free heme induces HO-1 expression in bone marrow (BM) and white blood (WB) cells, via a mechanism involving Nrf2. Heme catabolism by HO-1 produces CO that prevents (STOP I) further heme release from the cell-free Hb after *Plasmodium* infection, suppressing the pathogenesis of ECM. Moreover, sickle human Hb exerts an immunoregulatory effect that appears to act independently of Nrf2 and/or HO-1 and that inhibits (STOP II) cytotoxic GrB^+CD8^+ T cells (T_C) activation and expansion. APC: Antigen presenting cell.

of ECM (Figures 6H and 6I)(Pamplona et al., 2007) (Figure 7). However, CO might have additional protective effects that contribute to prevent the lethal outcome of *Plasmodium* infection (Ferreira et al., 2008).

Other end-products of heme catabolism by HO-1, such as labile iron, might also contribute to the protective effect conferred by sickle Hb against malaria. While cytotoxic *per se*, labile iron induces the expression of ferritin H chain (FtH)(Berberat et al., 2003; Eisenstein et al., 1991), which confers cytoprotection against free heme in vitro (Balla et al., 1992). We have obtained preliminary evidence suggesting that the cytoprotective effect of FtH is required to support the salutary effects of HO-1 (Seixas et al., 2009) against the onset of noncerebral forms of severe malaria in mice (Raffaella Gozzelino, personal communication.

The pathogenesis of ECM relies on a ''multiple hit'' system in which free heme synergizes with other cytotoxic agonists, e.g. pathogenic $CD8^+$ T cells, to trigger disease onset (Ferreira et al., 2008; Pamplona et al., 2007). While sickle Hb suppresses both, accumulation of pathogenic free heme (Figure 6A) and activation and/or expansion of pathogenic $CD8^+$ T cells (Figure 4D and e), it appears to do so via different mechanisms. Namely, it inhibits the accumulation of free heme after infection, via the HO-1/CO system (Figures 6A and G) while restraining the activation and/or expansion of pathogenic $CD8^+$ T cells (Figure 4D), via a mechanism that does not seem to involve HO-1 (Figure 4D and e, Figure S9) or Nrf2 (Figure S10). This latter effect is in keeping with the likely immunoregulatory basis of the protective effect of sickle cell trait against severe malaria in human populations (Williams et al., 2005a). While the immunoregulatory effect of sickle Hb appears to be driven by free heme (Figure S12) its molecular mechanism acts via a signal transduction pathway that remains to be established and that might target antigen presenting cells, e.g. dendritic cells, and/or $CD8^+$ T cells.

Its is possible that chronic hemolysis, associated with oxidation of cell-free Hb and production of circulating free heme, acts as a general protective mechanism against severe forms of malaria in human populations. This would contribute to explain the survival advantage conferred by a variety of RBC mutations against *P. falciparum* infection. In keeping with this notion, many of these RBC mutations can induce hemolysis (spontaneously or upon oxidative challenge) associated with the accumulation of circulating free heme (Muller-Eberhard et al., 1968). Some of these also afford protection against CM as illustrated for HbC (May et al., 2007; Modiano et al., 2001), glucose 6 phosphate dihydrogenase (G6PD) deficiency in males (Guindo et al., 2007), β- or α-thalassemia that confer protection mainly against severe anemia caused by *P. falciparum* infection (May et al., 2007) as well as other RBC cytoskeleton or membrane protein defects (Williams, 2006). The notion that chronic hemolysis might be protective *per se* against severe forms of malaria is strongly supported by the observation that heme administration to naïve mice, is sufficient *per se* to elicit a protective response (Figure 6D and Figure S12), relying, presumably on the induction of the Nrf2/HO-1 system. This is however, difficult to prove because the same Nrf2/HO-1 system provides protection against the pathological outcome of some of these RBC mutations, as demonstrated for sickle cell disease (Belcher et al., 2006).

In conclusion, we suggest that induction of the Nrf2/HO-1 system associated with sickle cell trait and probably with other often clinically silent genetic RBC defects might provide a general protective mechanism against *Plasmodium* infection in human populations. We propose that modulation of the Nrf2/HO-1 system might be used therapeutically to treat severe forms of malaria and in particular CM.

EXPERIMENTAL PROCEDURES

Mice

C57BL/6 *Hmox1*$^{+/-}$ mice were provided by Shaw-Fang Yet (Brigham and Women's Hospital, Boston)(Yet et al., 1999). C57BL/6 *Nrf2*$^{-/-}$ mice were provided by the RIKEN BioResource Center (Koyadai, Tsukuba, Ibaraki, Japan)(Itoh et al., 1997). C57BL/6 Hb^{SAD} mice were provided by Annie Henri (INSERM U733 IUH Hôpital Saint-Louis, Paris)(Trudel et al., 1991). C57BL/6.Sv129 $Hb^{A/A}$ mice were provided by Tim M. Townes and Tom M. Ryan (University of Alabama at Birmingham, USA)(Wu et al., 2006). $Hb^{A/a}$ mice expressing one copy of the human Hb chains (Hb^A) and one copy of the endogenous mouse Hb chains (Hb^a) were produced from C57BL/6.Sv129 $Hb^{A/A}$ x C57BL/6 Hb^{wt} mice (or C57BL/6 $Hb^{a/a}$) breeding. Mice were genotyped by PCR (*Hmox1* and *Nrf2*) and isoelectric focusing (*Hb*), as described elsewhere (Pamplona et al., 2007; Trudel et al., 1991). Experimental protocols were approved by the ''Instituto Gulbenkian de Ciência animal care committee''

and by the "Direcção Geral de Veterenária (DGV)" of the Portuguese Ministry of Agriculture, Rural Development and Fisheries (License 018831-2010-09-03).

Bone Marrow Chimeras

Bone marrow chimeras were generated in *Hmox1*$^{+/+}$, *Hmox1*$^{+/-}$ mice expressing or not the *Hb*^{SAD} allele (8–10 weeks) as described (Seixas et al., 2009).

Parasites, Infection, and Disease assessment

Mice were infected with (GFP)-*P. berghei* ANKA (Pamplona et al., 2007), GFP-Luciferase *P. berghei* ANKA (MR4-866) or a (GFP)-*P. berghei* transgenic parasite expressing different MHC II and MHC I restricted epitopes including the MHC I-restricted epitope derived from glycoprotein B of herpes simplex virus-1 ($gB_{498-505}$)(Lundie et al., 2008), provided by William R. Heath (Walter and Eliza Hall, Melbourne, Victoria, Australia). Parasitemias were determined by flow cytometry (Pamplona et al., 2007). Infected mice were monitored twice daily for clinical symptoms of ECM.

Visualization and Quantification of Luciferase Activity *P. berghei* ANKA Infected Mice

Luciferase activity was visualized by imaging of dissected tissues using an electron multiplying-charge-coupled device (EM-CCD) photon-counting camera (ImagEM, Hamamatsu).

Protoporphyrins

Iron-protoporphyrin IX (FePPIX; heme) and zinc-protoporphyrin IX (ZnPPIX) were dissolved in 0.2 M NaOH, neutralized (pH 7.4) with 0.2 M HCl and administered (i.p.), as described (Pamplona et al., 2007).

CO Treatment

Mice were placed in a gastight 60 L capacity chamber and exposed continuously between days 4–7 postinfection to CO at a flow rate of ~12 L/min (final concentration of 250 parts per million; ppm), as described (Pamplona et al., 2007; Sato et al., 2001). CO concentration was monitored using a CO analyzer (Interscan Corporation, Chatsworth).

Histology

Brains were harvested, when clinical signs of ECM were noticed in control mice. Tissue was fixed in buffered 4% (vol/vol) paraformaldehyde and histological analysis was performed on perfusion-fixed tissues.

BBB Permeability

Mice were injected intravenously (i.v.) with 0.1 ml of 2% Evans Blue (Sigma) when clinical symptoms of ECM were noticed in control mice (Pamplona et al., 2007).

Analyzes of Splenic CD8$^+$ T Cell Activation

Intracellular granzyme B staining were performed as described elsewhere (Lundie et al., 2008). Analyzes of CD8$^+$ T cells recognizing the MHC I-restricted epitope $gB_{498-505}$ (SSIEFARL) from glycoprotein B of herpes simplex virus-1, was performed as described elsewhere (Lundie et al., 2008).

Leukocyte Brain Infiltration

Leukocytes were isolated from the brain of *P. berghei* ANKA infected mice when clinical symptoms of ECM were detectable in control groups. Brain leukocyte infiltration was quantified by flow cytometry (Pamplona et al., 2007).

Quantitative Real-Time Reverse Transcription PCR

Mice were sacrificed at day ECM onset in *Hb*^{wt} mice. *Hmox1* mRNA was quantified by Quantitative real-time reverse transcription PCR (qRT-PCR) (Roche System)(Pamplona et al., 2007). TaqMan® Gene Signature Mouse Immune Array (Applied Biosystems) was used to quantify all other mRNAs (7900HT ABI system), according to manufactures recommendations.

Serum Biochemistry

Hematograms were measured by focused flow technology (Hemavet Multispecies Hematology System, HV950FS, Drew Scientific Inc., Centro Diagnóstivo Veterinário, Lisboa, Portugal). Plasma Hb was determined by spectroscopy at λ=577. Total plasma heme was measured using the 3,3′, 5,5′ tetramethylbenzidine (TMB) peroxidase assay (BD Biosciences), at λ=655 nm.

Statistical Analysis

Nonparametric Mann-Whitney *U* test was used to assess statistical significance between averages in different samples in which $n<5$. In samples with $n \geq 5$ the unpaired Student's *t*-test for unequal variances was used. Normal distributions were confirmed using the Kolmogorov-Smirnov test. Significant differences in survival were evaluated by the generation of Kaplan-Meier plots and by performing log-rank analysis for all experiments in which survival was assessed as an end-point. Statistical analysis for the progeny-expected ratios was performed using Pearson's chi-squared tests. $^*P<0.05$ or $^{**}P<0.01$ were considered statistically significant.

SUPPLEMENTAL INFORMATION

Supplemental Information includes Extended Experimental Procedures, twelve figures, and two tables and can be found with this article online at doi:10.1016/j.cell.2011.03.049.

ACKNOWLEDGMENTS

We thank Ruslan Medzhitov for intellectual support and encouragement by means of many insightful discussions, Thiago Carvalho (Instituto Gulbenkian de Ciê ncia) and Rui Costa Fundação Champalimaud as well as Marcelo Bozza (Universidade Federal do Rio De Janeiro), Robert P. Hebbel and Gregory Vercellotti (University of Minnesota, USA) for critical review of the manuscript, Nuno Sepúlveda for support in statistical analysis, Tim M. Townes and Tom M. Ryan (University of Alabama at Birmingham) for providing the HbA/A mice. Sílvia Cardoso and Matteo Villa for mouse breeding and genotyping. This work was supported by "*Fundação para a Ciência e a Tecnologia*", Portugal grants PTDC/SAU-MII/71140/2006 and SFRH/BPD/21707/2005 (AF), SFHR/BD/33218/2007 (IM), PTDC/SAU-MII/71140/2006, PTDC/BIA-BCM/101311/2008, PTDC/SAU-FCF/100762/2008, GEMI Fund Linde Healthcare, European Community and LSH-2005-1.2.5-1 (MPS), FP7-PEOPLE-2007-2-1-IEF (VJ). I.B. is supported by the DFG, BMBF, Dr. Senckenberg-Stiftung, Kassel-Stiftung and Messer-Stiftung, Germany. Annie Henri is supported by INSERM and Yves Beuzard by Paris VII University, Commissariat à l'Énergie Atomique and Agence Nationale de la Recherche Scientifique, France.

Author contribution: A.F. contributed to study design, performed and/or contributed critically to all experiments, analyzed data and was assisted to do so by NRP. A.C. performed experiments and analysis of leukocyte infiltration and generation of bone marrow chimeric animals with A.F. I.M.: performed experiments and interpreted data revealing the immunoregulatory effect of sickle hemoglobin with A.F. I.B. provided expert analysis, advice and teaching on immunopathology. V.J. determined free heme concentrations in plasma and quantified HO activity. S.R. generated and maintained all mouse colonies used. A.H. provided the *Hb*^{SAD} mice. YB provided mentorship and advise on sickle cell mouse model. M.P.S. formulated the original hypothesis, drove most of the study design, analyzed and provided mentorship. The manuscript was written by M.P.S. with assistance from A.F. and Y.B.

Received: June 21, 2010
Revised: January 3, 2011
Accepted: March 28, 2011
Published: April 28, 2011

REFERENCES

Alam, J., Stewart, D., Touchard, C., Boinapally, S., Choi, A.M., and Cook, J.L. (1999). Nrf2, a Cap'n'Collar transcription factor, regulates induction of the heme oxygenase-1 gene. J. Biol. Chem. *274*, 26071–26078.

Allison, A.C. (1954). Protection afforded by sickle-cell trait against subtertian malareal infection. BMJ *1*, 290–294.

Ayi, K., Turrini, F., Piga, A., and Arese, P. (2004). Enhanced phagocytosis of ring-parasitized mutant erythrocytes: a common mechanism that may explain protection against falciparum malaria in sickle trait and beta-thalassemia trait. Blood *104*, 3364–3371.

Bains, S.K., Foresti, R., Howard, J., Atwal, S., Green, C.J., and Motterlini, R. (2010). Human sickle cell blood modulates endothelial heme oxygenase activity: effects on vascular adhesion and reactivity. Arterioscler. Thromb. Vasc. Biol. *30*, 305–312.

Balla, G., Jacob, H.S., Balla, J., Rosenberg, M., Nath, K., Apple, F., Eaton, J.W., and Vercellotti, G.M. (1992). Ferritin: a cytoprotective antioxidant strategem of endothelium. J. Biol. Chem. *267*, 18148–18153.

Beet, E.A. (1947). Sickle cell disease in Northern Rhodesia. East Afr. Med. J. *24*, 212–222.

Belcher, J.D., Mahaseth, H., Welch, T.E., Otterbein, L.E., Hebbel, R.P., and Vercellotti, G.M. (2006). Heme oxygenase-1 is a modulator of inflammation and vaso-occlusion in transgenic sickle mice. J. Clin. Invest. *116*, 808–816.

Belnoue, E., Kayibanda, M., Vigario, A.M., Deschemin, J.C., van Rooijen, N., Viguier, M., Snounou, G., and Renia, L. (2002). On the pathogenic role of brain-sequestered alphabeta CD8+ T cells in experimental cerebral malaria. J. Immunol. *169*, 6369–6375.

Berberat, P.O., Katori, M., Kaczmarek, E., Anselmo, D., Lassman, C., Ke, B., Shen, X., Busuttil, R.W., Yamashita, K., Csizmadia, E., et al. (2003). Heavy chain ferritin acts as an antiapoptotic gene that protects livers from ischemia reperfusion injury. FASEB J. *17*, 1724–1726.

Campanella, G.S., Tager, A.M., El Khoury, J.K., Thomas, S.Y., Abrazinski, T.A., Manice, L.A., Colvin, R.A., and Luster, A.D. (2008). Chemokine receptor CXCR3 and its ligands CXCL9 and CXCL10 are required for the development of murine cerebral malaria. Proc. Natl. Acad. Sci. USA *105*, 4814–4819.

Clark, I.A., Alleva, L.M., Mills, A.C., and Cowden, W.B. (2004). Pathogenesis of malaria and clinically similar conditions. Clin. Microbiol. Rev. *17*, 509–539.

Crompton, P.D., Traore, B., Kayentao, K., Doumbo, S., Ongoiba, A., Diakite, S.A., Krause, M.A., Doumtabe, D., Kone, Y., Weiss, G., et al. (2008). Sickle cell trait is associated with a delayed onset of malaria: implications for time-to-event analysis in clinical studies of malaria. J. Infect. Dis. *198*, 1265–1275.

Eisenstein, R.S., Garcia, M.D., Pettingell, W., and Munro, H.N. (1991). Regulation of ferritin and heme oxygenase synthesis in rat fibroblasts by different forms of iron. Proc. Natl. Acad. Sci. USA *88*, 688–692.

Ferreira, A., Balla, J., Jeney, V., Balla, G., and Soares, M.P. (2008). A central role for free heme in the pathogenesis of severe malaria: the missing link? J. Mol. Med. *86*, 1097–1111.

Friedman, M.J. (1978). Erythrocytic mechanism of sickle cell resistance to malaria. Proc. Natl. Acad. Sci. USA *75*, 1994–1997.

Gozzelino, R., Jeney, V., and Soares, M.P. (2010). Mechanisms of cell protection by heme oxygenase-1. Annu. Rev. Pharmacol. Toxicol. *50*, 323–354.

Guindo, A., Fairhurst, R.M., Doumbo, O.K., Wellems, T.E., and Diallo, D.A. (2007). X-linked G6PD deficiency protects hemizygous males but not heterozygous females against severe malaria. PLoS Med. *4*, e66.

Hebbel, R.P., Morgan, W.T., Eaton, J.W., and Hedlund, B.E. (1988). Accelerated autoxidation and heme loss due to instability of sickle hemoglobin. Proc. Natl. Acad. Sci. USA *85*, 237–241.

Hood, A.T., Fabry, M.E., Costantini, F., Nagel, R.L., and Shear, H.L. (1996). Protection from lethal malaria in transgenic mice expressing sickle hemoglobin. Blood *87*, 1600–1603.

Hutagalung, R., Wilairatana, P., Looareesuwan, S., Brittenham, G.M., Aikawa, M., and Gordeuk, V.R. (1999). Influence of hemoglobin E trait on the severity of Falciparum malaria. J. Infect. Dis. *179*, 283–286.

Itoh, K., Chiba, T., Takahashi, S., Ishii, T., Igarashi, K., Katoh, Y., Oyake, T., Hayashi, N., Satoh, K., Hatayama, I., et al. (1997). An Nrf2/small Maf heterodimer mediates the induction of phase II detoxifying enzyme genes through antioxidant response elements. Biochem. Biophys. Res. Commun. *236*, 313–322.

Jallow, M., Teo, Y.Y., Small, K.S., Rockett, K.A., Deloukas, P., Clark, T.G., Kivinen, K., Bojang, K.A., Conway, D.J., Pinder, M., et al. (2009). Genome-wide and fine-resolution association analysis of malaria in West Africa (Nat Genet).

Jison, M.L., Munson, P.J., Barb, J.J., Suffredini, A.F., Talwar, S., Logun, C., Raghavachari, N., Beigel, J.H., Shelhamer, J.H., Danner, R.L., et al. (2004). Blood mononuclear cell gene expression profiles characterize the oxidant, hemolytic, and inflammatory stress of sickle cell disease. Blood *104*, 270–280.

Kensler, T.W., Wakabayashi, N., and Biswal, S. (2007). Cell survival responses to environmental stresses via the Keap1-Nrf2-ARE pathway. Annu. Rev. Pharmacol. Toxicol. *47*, 89–116.

Larsen, R., Gozzelino, R., Jeney, V., Tokaji, L., Bozza, F.A., Japiassu, A.M., Bonaparte, D., Cavalcante, M.M., Chora, A., Ferreira, A., et al. (2010). A central role for free heme in the pathogenesis of severe sepsis. Sci Transl Med *2*, 51ra71.

Livincstone, F.B. (1971). Malaria and human polymorphisms. Annu. Rev. Genet. *5*, 33–64.

Lundie, R.J., de Koning-Ward, T.F., Davey, G.M., Nie, C.Q., Hansen, D.S., Lau, L.S., Mintern, J.D., Belz, G.T., Schofield, L., Carbone, F.R., et al. (2008). Blood-stage Plasmodium infection induces CD8+ T lymphocytes to parasite-expressed antigens, largely regulated by CD8alpha+ dendritic cells. Proc. Natl. Acad. Sci. USA *105*, 14509–14514.

May, J., Evans, J.A., Timmann, C., Ehmen, C., Busch, W., Thye, T., Agbenyega, T., and Horstmann, R.D. (2007). Hemoglobin variants and disease manifestations in severe falciparum malaria. JAMA *297*, 2220–2226.

Mishra, S.K., and Newton, C.R. (2009). Diagnosis and management of the neurological complications of falciparum malaria. Nat Rev Neurol *5*, 189–198.

Modiano, D., Luoni, G., Sirima, B.S., Simpore, J., Verra, F., Konate, A., Rastrelli, E., Olivieri, A., Calissano, C., Paganotti, G.M., et al. (2001). Haemoglobin C protects against clinical Plasmodium falciparum malaria. Nature *414*, 305–308.

Motulsky, A.G., Vandepitte, J., and Fraser, G.R. (1966). Population genetic studies in the Congo. I. Glucose-6-phosphate dehydrogenase deficiency, hemoglobin S, and malaria. Am. J. Hum. Genet. *18*, 514–537.

Muller-Eberhard, U., Javid, J., Liem, H.H., Hanstein, A., and Hanna, M. (1968). Plasma concentrations of hemopexin, haptoglobin and heme in patients with various hemolytic diseases. Blood *32*, 811–815.

Nath, K.A., Balla, G., Vercellotti, G.M., Balla, J., Jacob, H.S., Levitt, M.D., and Rosenberg, M.E. (1992). Induction of heme oxygenase is a rapid, protective response in rhabdomyolysis in the rat. J. Clin. Invest. *90*, 267–270.

Nath, K.A., Grande, J.P., Haggard, J.J., Croatt, A.J., Katusic, Z.S., Solovey, A., and Hebbel, R.P. (2001). Oxidative stress and induction of heme oxygenase-1 in the kidney in sickle cell disease. Am. J. Pathol. *158*, 893–903.

Ogawa, K., Sun, J., Taketani, S., Nakajima, O., Nishitani, C., Sassa, S., Hayashi, N., Yamamoto, M., Shibahara, S., Fujita, H., et al. (2001). Heme mediates derepression of Maf recognition element through direct binding to transcription repressor Bach1. EMBO J. *20*, 2835–2843.

Pamplona, A., Ferreira, A., Balla, J., Jeney, V., Balla, G., Epiphanio, S., Chora, A., Rodrigues, C.D., Gregoire, I.P., Cunha-Rodrigues, M., et al. (2007). Heme oxygenase-1 and carbon monoxide suppress the pathogenesis of experimental cerebral malaria. Nat. Med. *13*, 703–710.

Pasvol, G., Weatherall, D.J., and Wilson, R.J. (1978). Cellular mechanism for the protective effect of haemoglobin S against P. falciparum malaria. Nature *274*, 701–703.

Raberg, L., Sim, D., and Read, A.F. (2007). Disentangling genetic variation for resistance and tolerance to infectious diseases in animals. Science *318*, 812–814.

Reiter, C.D., Wang, X., Tanus-Santos, J.E., Hogg, N., Cannon, R.O., 3rd, Schechter, A.N., and Gladwin, M.T. (2002). Cell-free hemoglobin limits nitric oxide bioavailability in sickle-cell disease. Nat. Med. *8*, 1383–1389.

Sabaa, N., de Franceschi, L., Bonnin, P., Castier, Y., Malpeli, G., Debbabi, H., Galaup, A., Maier-Redelsperger, M., Vandermeersch, S., Scarpa, A., et al. (2008). Endothelin receptor antagonism prevents hypoxia-induced mortality

and morbidity in a mouse model of sickle-cell disease. J. Clin. Invest. *118*, 1924–1933.

Sato, K., Balla, J., Otterbein, L., Snith, N.R., Brouard, S., Lin, Y., Czismadia, E., Sevigny, J., Robson, S.C., Vercellotti, G., et al. (2001). Carbon monoxide generated by heme oxygenase-1 suppresses the rejection of mouse to rat cardiac transplants. J. Immunol. *166*, 4185–4194.

Schneider, D.S., and Ayres, J.S. (2008). Two ways to survive infection: what resistance and tolerance can teach us about treating infectious diseases. Nat. Rev. Immunol. *8*, 889–895.

Schofield, L., and Grau, G.E. (2005). Immunological processes in malaria pathogenesis. Nat. Rev. Immunol. *5*, 722–735.

Sears, D.A., Udden, M.M., and Thomas, L.J. (2001). Carboxyhemoglobin levels in patients with sickle-cell anemia: relationship to hemolytic and vasoocclusive severity. Am. J. Med. Sci. *322*, 345–348.

Seixas, E., Gozzelino, R., Chora, A., Ferreira, A., Silva, G., Larsen, R., Rebelo, S., Penido, C., Smith, N.R., Coutinho, A., et al. (2009). Heme oxygenase-1 affords protection against noncerebral forms of severe malaria. Proc. Natl. Acad. Sci. USA *106*, 15837–15842.

Shear, H.L., Roth, E.F., Jr., Fabry, M.E., Costantini, F.D., Pachnis, A., Hood, A., and Nagel, R.L. (1993). Transgenic mice expressing human sickle hemoglobin are partially resistant to rodent malaria. Blood *81*, 222–226.

Soares, M.P., and Bach, F.H. (2009). Heme oxygenase-1: from biology to therapeutic potential. Trends Mol. Med. *15*, 50–58.

Tenhunen, R., Marver, H.S., and Schmid, R. (1968). The enzymatic conversion of heme to bilirubin by microsomal heme oxygenase. Proc. Natl. Acad. Sci. USA *61*, 748–755.

Trudel, M., De Paepe, M.E., Chretien, N., Saadane, N., Jacmain, J., Sorette, M., Hoang, T., and Beuzard, Y. (1994). Sickle cell disease of transgenic SAD mice. Blood *84*, 3189–3197.

Trudel, M., Saadane, N., Garel, M.C., Bardakdjian-Michau, J., Blouquit, Y., Guerquin-Kern, J.L., Rouyer-Fessard, P., Vidaud, D., Pachnis, A., Romeo, P.H., et al. (1991). Towards a transgenic mouse model of sickle cell disease: hemoglobin SAD. EMBO J. *10*, 3157–3165.

Williams, T.N. (2006). Human red blood cell polymorphisms and malaria. Curr. Opin. Microbiol. *9*, 388–394.

Williams, T.N., Mwangi, T.W., Roberts, D.J., Alexander, N.D., Weatherall, D.J., Wambua, S., Kortok, M., Snow, R.W., and Marsh, K. (2005a). An immune basis for malaria protection by the sickle cell trait. PLoS Med. *2*, e128.

Williams, T.N., Mwangi, T.W., Wambua, S., Alexander, N.D., Kortok, M., Snow, R.W., and Marsh, K. (2005b). Sickle cell trait and the risk of Plasmodium falciparum malaria and other childhood diseases. J. Infect. Dis. *192*, 178–186.

Wu, L.C., Sun, C.W., Ryan, T.M., Pawlik, K.M., Ren, J., and Townes, T.M. (2006). Correction of sickle cell disease by homologous recombination in embryonic stem cells. Blood *108*, 1183–1188.

Yet, S.F., Perrella, M.A., Layne, M.D., Hsieh, C.M., Maemura, K., Kobzik, L., Wiesel, P., Christou, H., Kourembanas, S., and Lee, M.E. (1999). Hypoxia induces severe right ventricular dilatation and infarction in heme oxygenase-1 null mice. Journal of Clinical Investigation *103*, R23–R29.

EXTENDED EXPERIMENTAL PROCEDURES

Mice

C57BL/6 *Hmox1*$^{+/-}$ mice were provided by Shaw-Fang Yet (Brigham and Women's Hospital, Boston)(Yet et al., 1999). C57BL/6 *Nrf2*$^{-/-}$ mice were obtained from the RIKEN BioResource Center (Koyadai, Tsukuba, Ibaraki, Japan)(Itoh et al., 1997). C57BL/6 *Hb*^{SAD} mice (expressing 19% *Hb*^{SAD}, i.e. $a^{H}{}_{2}\beta_{2}{}^{SAD}$) were provided originally by Annie Henri (INSERM U733 IUH Hôpital Saint-Louis, Paris)(-Trudel et al., 1991). The transgenic *Hb*^{SAD} mice used in this study are hemizygotes for a cluster of human genes including one copy the Hb β SAD gene and two copies of α gene (Trudel et al., 1994). The insertion site of this cluster in the mouse genome was not determined. The human α globin chains represent about 50% of the total α chain content, while the β SAD chain is only 19% of the total β chains. These human chains are not expressed in addition to the mouse globin chains but at their expense. The ratio of α/β globin chain synthesis remains normal. The relative excess in human α globin chains (compared to the β SAD chains) form functional human α/β mouse hybrid Hb. The Hb content in RBC remains normal and RBC survival is not affected (normal reticulocyte counts)(*Suppl. Table 1a*). The various blood counts are in the normal range (*Suppl. Table 1a*). However, SAD RBC exhibit a slight dehydration, which revealed by an increase in the intracellular Hb concentration (MCHC)(*Suppl. Table 1a*). This is expected from the presence of *Hb*^{SAD} (loss of 3 negative charges and an increased isoelectric charge). This modest modification is also seen in Hb C heterozygote state in human and it plays a role in the S/C syndrome when associated with the S determinant in compound heterozygote. While hemizygous *Hb*^{SAD} can develop typical complications of sickle cell disease, e.g. generalized congestion and microvascular occlusions, occasionally with thrombosis and infarctions of lung, kidneys, penis and myocardium these occur only when *Hb*^{SAD} mice are exposed to hypoxia or upon extensive aging, i.e. 38-75 weeks (Trudel et al., 1994). *Hb*^{SAD} neonates exhibit transient anemia at delivery, related to hemolysis caused by *Hb*^{SAD} polymerization, most probably due to transient hypoxia associated with late fetal development and delivery. Hb values in *Hb*^{SAD} mice return to normal levels shortly after weaning (Trudel et al., 1991). *Hb*^{SAD} mice used in the experiments described hereby were under the age of 18 weeks presenting no overt hematological changes (*Suppl. Table 1a*) or complications of sickle cell disease. *Hb*^{SAD}*Hmox1*$^{+/-}$ and *Hb*^{SAD}*Nrf2*$^{+/-}$ mice were generated from *Hb*^{SAD}*Hmox1*$^{+/-}$ x *Hb*^{wt} *Hmox1*$^{+/-}$ or *Hb*^{SAD}*Nrf2*$^{+/-}$ x *Hb*^{wt}Nrf2$^{+/-}$ breeding, respectively (*Suppl. Table 2*). C57BL/6.Sv129 *Hb*$^{A/A}$ mice, a knock-in mouse model expressing exclusively human Hb without the endogenous mouse Hb were provided originally by Tim Townes (University of Alabama at Birmingham, USA)(Wu et al., 2006). *Hb*$^{A/A}$ mice present normal RBC morphology and hematologic parameters (Wu et al., 2006). Breeding of the *Hb*$^{A/A}$ with C57BL/6 *Hb*^{wt} mice (or C57BL/6 *Hb*$^{a/a}$) resulted in the production of *Hb*$^{A/a}$ mice, expressing only one copy of the human Hb chains (*Hb*^{A}) and one copy of the endogenous mouse Hb chains (*Hb*^{a}). Interbreeding of *Hb*$^{A/a}$ mice produced, among other genotypes, *Hb*$^{A/a}$ mice and littermate control *Hb*$^{a/a}$ mice expressing only the endogenous alleles of the mouse Hb chains. Both genotypes, i.e. *Hb*$^{A/a}$ and *Hb*$^{a/a}$ mice, presented regular Hb levels, 11.0 ± 0.5 and 12.1 ± 0.9 (g/dl), respectively; hematocrit, 40.1 ± 2.5 and 41.8 ± 2.6 (%), respectively and RBC counts, 8.6 ± 0.5 and 8.3 ± 0.6 (x10^{6}/μL), respectively, but decreased levels of Mean Cell Hemoglobin content (MCHC), 27.5 ± 2.0 and 28.8 ± 1.4 (g/dl), respectively. Mice were genotyped by PCR (*Hmox1* and *Nrf2*) and isoelectric focusing (*Hb*), as described elsewhere (Pamplona et al., 2007; Trudel et al., 1991). Experimental protocols were approved by the "Instituto Gulbenkian de Ciência animal care committee" and by the "Direcção Geral de Veterenária (DGV)" of the Portuguese Ministry of Agriculture, Rural Development and Fisheries (License 018831-2010-09-03).

Bone Marrow Chimeras

Bone Marrow chimeras were generated in *Hmox1*$^{+/+}$, *Hmox1*$^{+/-}$ mice expressing or not the *Hb*^{SAD} allele (8-10 weeks). Mice (recipients) were lethally irradiated (900 rad, 2.35 minutes, 137Cs source)(Gammacell 2000, Mølsgaard Medical, Denmark) and reconstituted 4 hours thereafter with 10^{6} total bone marrow cells from *Hmox1*$^{+/+}$, *Hmox1*$^{+/-}$ expressing or not the *Hb*^{SAD} allele (6 weeks). Chimerism was assessed 8-10 weeks thereafter by RT-PCR, as described (Seixas et al., 2009). Flow cytometry was used to assess percent and total number of circulating cells in reconstituted mice as compared to control nonchimeric mice.

Parasites, Infection, and Disease Assessment

Mice were infected by intraperitoneal (i.p.) inoculation of 10^{5} RBCs infected with (GFP)-*P. berghei* ANKA (Pamplona et al., 2007), GFP-Luciferase *P. berghei* ANKA (MR4-866) or a (GFP)-*P. berghei* transgenic parasite expressing different MHC II and MHC I restricted epitopes including the MHC I-restricted epitope derived from glycoprotein B of herpes simplex virus-1 ($gB_{498-505}$)(Lundie et al., 2008), provided originally by William R. Heath (Walter and Eliza Hall, Melbourne, Victoria, Australia). Drug-resistant *P. berghei* ANKA transfectants were selected using Pyrimethamine (10 mg/ml in drinking water). Parasitemias were determined by flow cytometry (Pamplona et al., 2007). Infected mice were monitored twice daily for clinical symptoms of ECM including hemi- or paraplegia, head deviation, tendency to roll-over on stimulation, ataxia and convulsions. All experiments were performed in mice sacrificed under CO_2 and perfused with PBS, at the time of ECM in control mice.

Visualization and Quantification of Luciferase Activity *P. berghei* ANKA Infected Mice

Luciferase activity was visualized by imaging of dissected tissues using an electron multiplying-charge-coupled device (EM-CCD) photon-counting camera (ImagEM, Hamamatsu). Mice received d-Luciferin (i.p.) in PBS (100 mg/kg of body weight; Promega) at day 7 postinfection, at the time of ECM onset. Mice were sacrificed and perfused with PBS 5 min thereafter. Organs were dissected,

placed in a Petri dish and exposed (5–120 s). Imaging quantification was performed with ImajeJ software and is expressed arbitrary units per mg of tissue.

Protoporphyrins

Iron-protoporphyrin IX (FePPIX; heme) and zinc-protoporphyrin IX (ZnPPIX) were dissolved in 0.2 M NaOH, neutralized (pH 7.4) with 0.2 M HCl and administered (i.p.), as described (Pamplona et al., 2007).

HO-1 Activity

Spleen and liver were harvested and snapfrozen in liquid nitrogen. Tissue samples were homogenized in 3 mL of homogenizing buffer (200 mM KH_2PO_4, 135 mM KCl, 0.1 mM EDTA, [pH 7.4]), and sonicated at 4°C. The supernatant was transferred to ultracentrifuge tubes and 5 mL of homogenizing buffer was added, followed by an ultracentrifugation (100.000*g*, 4°C, 1h, Beckman L7-35 Ultracentrifuge, 70 Ti rotor). The microsomal pellet was resuspended in 320 ml of HO activity buffer (100 mM KH_2PO_4, 2 mM $MgCl_2$, [pH 7.4]). Samples were sonicated again, centrifuged and the supernatant was used to determine HO activity using rat liver cytosol (as a source of biliverdin reductase, 2 mg/assay), hemin (20 mM), glucose 6-phosphate (2 mM), glucose 6-phosphate dehydrogenase (0.2 U/reaction) and NADPH (0.8 mM) (400 μl. 37 ^{0}C, 1 hr). Bilirubin was extracted (1 ml of chloroform; vortexing 3 × for 10 sec.). After centrifugation optical densities at λ=464 nm and λ=530 nm of the organic phase were determined and HO activity was calculated as pmol bilirubin formed/mg of tissue/hour.

CO treatment

Mice were placed in a gastight 60 L capacity chamber and exposed continuously between days 4-7 postinfection to CO at a flow rate of ~12 L/min (final concentration of 250 parts per million; ppm), as described (Pamplona et al., 2007; Sato et al., 2001). CO concentration was monitored using a CO analyzer (Interscan Corporation, Chatsworth).

Histology

Brains were harvested, when clinical signs of ECM were noticed in control mice. Tissue was fixed in buffered 4% (vol/vol) paraformaldehyde and histological analysis was performed on perfusion-fixed tissues.

BBB Permeability

Mice were injected intravenously (i.v.) with 0.1 ml of 2% Evans Blue (Sigma) when clinical symptoms of ECM were noticed in control mice. Mice were sacrificed 1h thereafter. Brains were weighted and placed in formamide (Merck) (37°C, 48h) to extract Evans Blue dye. Absorbance was measured at λ=620 nm (Spectronic Unicam, Heλios β). Evans Blue concentration was calculated from a standard curve of Evans Blue and is expressed as μg of Evans Blue *per* g of brain tissue (Pamplona et al., 2007).

Analyzes of splenic CD8$^+$ T cell activation

Single cell suspensions were obtained from spleen of naïve mice or five days after infection with a transgenic *P. berghei* ANKA strain encoding the MHC I-restricted epitope derived from the glycoprotein B of herpes simplex virus-1 ($gB_{498-505}$) (Lundie et al., 2008). For intracellular granzyme B staining splenocytes ($1x10^6$) were re-stimulated *in vitro* (5 hours, 37°C) with 100ng/ml of phorbol 12-myristate 13-acetate (Sigma), 500ng/ml Ionomycin (Calbiochem) in the presence of 10μg/ml brefeldin A (Epicenter Technologies). Fc receptors were blocked using anti-FcγIII/II (2.4G2) receptor antibody (produced in house) and cells were stained with anti-CD8 antibody (YTS169.4 clone, produced in house). Cells were fixed (2% paraformaldehyde in PBS, 30 min, RT) and permeabilized (0,5% saponin in PBS 2% FCS, 0 min, RT) prior to the addition of anti-granzyme B antibody (16G6 clone, eBioscience) in 0,5% saponin in PBS 2% FCS (30 min, RT). For the analyzes of CD8$^+$ T cells recognizing the MHC I-restricted epitope $gB_{498-505}$ (SSIEFARL) from glycoprotein B of herpes simplex virus-1, splenocytes ($2x10^6$) were stained with R-phycoerythrin-conjugated H-$2K^b$-$gB_{498–505}$ pentamer (ProImmune) according to manufacturer instructions prior to staining with anti-CD19 (MB19-1, eBioscience) and anti-CD8 antibodies. H-$2K^b$-$gB_{498–505}$ pentamer positive cells were determined as $CD19^-CD8^+$H-$2K^b$-$gB_{498–505}{}^+$. Data were acquired using FACSCalibur (BD Bioscience) and CyAn ADP (Dako Cytomation) and analyzed using FlowJo software (Tree Star Inc.). Dead cells were excluded from analysis based on propidium iodide staining.

Leukocyte Brain Infiltration

Leukocytes were isolated from the brain of *P. berghei* ANKA infected mice when clinical symptoms of ECM were detectable in control groups. Mice were perfused with PBS *in toto*, brains were collected, homogenized, digested (30 min, 37°C) in Hanks-balanced salt solution (HBSS; Life Technologies) supplemented with 0.2 mg/ml collagenase VIII (Sigma-Aldrich), strained (100 μm) (Becton Dickinson) and centrifuged (1200 g; 10 min). Brain leukocyte infiltration was quantified by flow cytometry (Pamplona et al., 2007).

Quantitative Real-Time Reverse Transcription PCR

Mice were sacrificed at day ECM onset in Hb^{wt} mice. RNA was isolated from brain, liver, kidney, heart, bone marrow, spleen and lungs using Trizol Reagent (Invitrogen, Life technologies) and RNeasy Plus Mini Kit (Quiagen), according to manufacturers recommendation. RNeasy Protect Animal Blood Kit (Quiagen) was used for the extraction of RNA from whole blood. cDNA was synthesized

as described (Pamplona et al., 2007). *Hmox1* mRNA was quantified by qRT-PCR (Roche System) as described (Pamplona et al., 2007). TaqMan Gene Signature Mouse Immune Array (Applied Biosystems) was used to quantify all other mRNAs (7900HT ABI system), according to manufactures recommendations.

Serum Biochemistry

Blood was collected in heparinized tubes by cardiac puncture, centrifuged (2x5min, 1600g). Hematograms were measured by focused flow technology (Hemavet Multispecies Hematology System, HV950FS, Drew Scientific Inc., CDVET Lab, Centro Diagnóstivo Veterinário, Lisboa, Portugal). Plasma Hb was determined by spectroscopy at λ=577. Total plasma heme was measured using the 3,3′, 5,5′ tetramethylbenzidine (TMB) peroxidase assay (BD Biosciences), at λ=655 nm. Purified Hb was used as standard for plasma Hb and heme measurements.

SUPPLEMENTAL REFERENCES

Itoh, K., Chiba, T., Takahashi, S., Ishii, T., Igarashi, K., Katoh, Y., Oyake, T., Hayashi, N., Satoh, K., Hatayama, I., et al. (1997). An Nrf2/small Maf heterodimer mediates the induction of phase II detoxifying enzyme genes through antioxidant response elements. Biochem Biophys Res Commun *236*, 313-322.

Lundie, R.J., de Koning-Ward, T.F., Davey, G.M., Nie, C.Q., Hansen, D.S., Lau, L.S., Mintern, J.D., Belz, G.T., Schofield, L., Carbone, F.R., et al. (2008). Blood-stage Plasmodium infection induces CD8+ T lymphocytes to parasite-expressed antigens, largely regulated by CD8alpha+ dendritic cells. Proc. Natl. Acad. Sci. USA *105*, 14509–14514.

Pamplona, A., Ferreira, A., Balla, J., Jeney, V., Balla, G., Epiphanio, S., Chora, A., Rodrigues, C.D., Gregoire, I.P., Cunha-Rodrigues, M., et al. (2007). Heme oxygenase-1 and carbon monoxide suppress the pathogenesis of experimental cerebral malaria. Nat. Med. *13*, 703–710.

Sato, K., Balla, J., Otterbein, L., Snith, N.R., Brouard, S., Lin, Y., Czismadia, E., Sevigny, J., Robson, S.C., Vercellotti, G., et al. (2001). Carbon monoxide generated by heme oxygenase-1 suppresses the rejection of mouse to rat cardiac transplants. J. Immunol. *166*, 4185–4194.

Seixas, E., Gozzelino, R., Chora, A., Ferreira, A., Silva, G., Larsen, R., Rebelo, S., Penido, C., Smith, N.R., Coutinho, A., et al. (2009). Heme oxygenase-1 affords protection against noncerebral forms of severe malaria. Proc. Natl. Acad. Sci. USA *106*, 15837–15842.

Trudel, M., De Paepe, M.E., Chretien, N., Saadane, N., Jacmain, J., Sorette, M., Hoang, T., and Beuzard, Y. (1994). Sickle cell disease of transgenic SAD mice. Blood *84*, 3189–3197.

Trudel, M., Saadane, N., Garel, M.C., Bardakdjian-Michau, J., Blouquit, Y., Guerquin-Kern, J.L., Rouyer-Fessard, P., Vidaud, D., Pachnis, A., Romeo, P.H., et al. (1991). Towards a transgenic mouse model of sickle cell disease: hemoglobin SAD. EMBO J. *10*, 3157–3165.

Wu, L.C., Sun, C.W., Ryan, T.M., Pawlik, K.M., Ren, J., and Townes, T.M. (2006). Correction of sickle cell disease by homologous recombination in embryonic stem cells. Blood *108*, 1183–1188.

Yet, S.F., Perrella, M.A., Layne, M.D., Hsieh, C.M., Maemura, K., Kobzik, L., Wiesel, P., Christou, H., Kourembanas, S., and Lee, M.E. (1999). Hypoxia induces severe right ventricular dilatation and infarction in heme oxygenase-1 null mice. J. Clin. Invest. *103*, R23–R29.

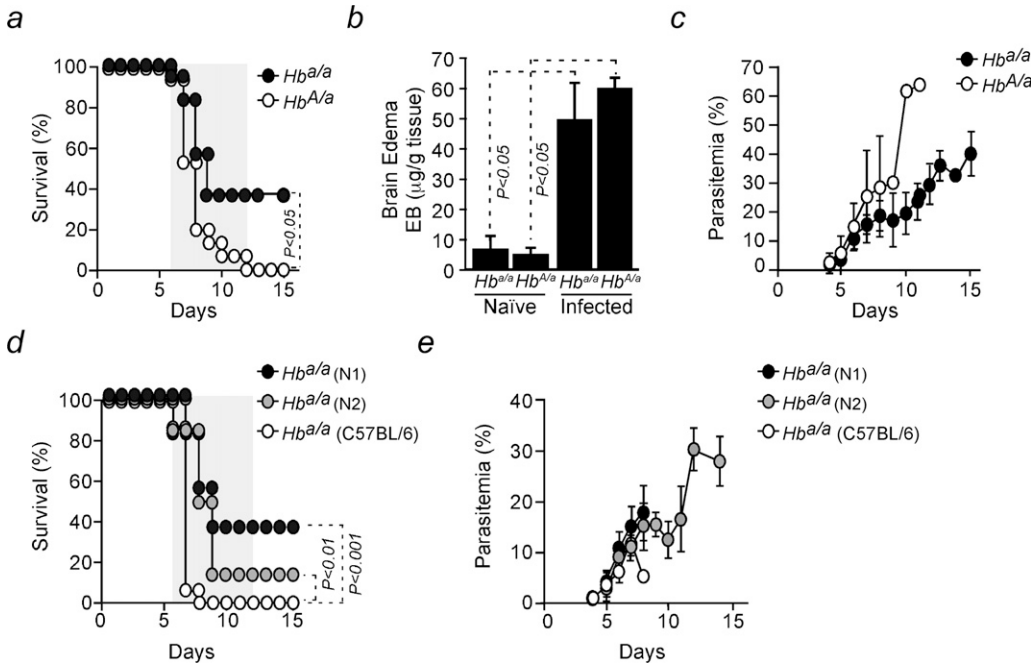

Figure S1. Hb$^{A/a}$ Mice Expressing Wild-Type Human Hb Are Not Protected against ECM, Related to Figure 1

(a) Survival of *P. berghei* ANKA-infected *Hb*$^{A/a}$ (n=15) and littermate control *Hb*$^{a/a}$ (n=19) mice (3 independent experiments with survival advantage P<0.05).

(b) Brain edema was measured by Evans blue (EB) accumulation in brains ± standard deviation (n=3-4/group), at the time of ECM onset in *Hb*$^{A/a}$ mice.

(c) Mean percentage of infected RBC ± standard deviation, same mice as in (*a*). Notice that the *Hb*$^{A/a}$ and *Hb*$^{a/a}$ mice used in these experiments are in a mixed C57BL/6.SV129 genetic background, produced by breeding *Hb*$^{A/a}$ mice.

(d) Survival of *P. berghei* ANKA-infected *Hb*$^{a/a}$ mice under different genetic backgrounds, i.e. *Hb*$^{a/a}$ N1 (n=19), *Hb*$^{a/a}$ N2 (n=7) and *Hb*$^{a/a}$ C57BL/6 (n=15) mice (data pooled from 4 independent experiments).

(e) Mean percentage of infected RBC in the same mice a sin (a). Grey shading indicates expected time of ECM. Notice that expression of a nonmutated β-chain of human Hb in the *Hb*$^{A/a}$ mice does not protect against ECM, as compared to littermate control *Hb*$^{a/a}$ mice. This supports the notion that protection of *Hb*^{SAD} mice against ECM is afforded by the mutations of β-chain of human Hb and not by the β-chain of human Hb itself.

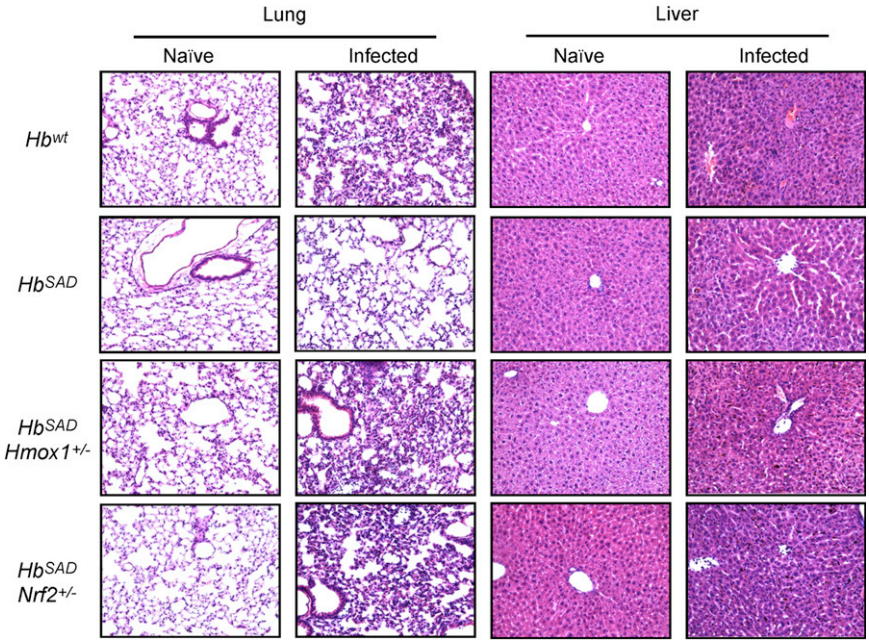

Figure S2. Hb^{SAD} Affords Protection against Lung and Liver Injury via a Mechanism Involving HO-1 and Nrf2, Related to Figures 1, 2, and 5

Paraffin sections stained with standard hematoxylin/eosin staining. Naïve Hb^{wt}, Hb^{SAD}, $Hb^{SAD}Hmox1^{+/-}$ and $Hb^{SAD}Nrf2^{+/-}$ mice exhibit normal lungs and livers that were indistinguishable from each other. Infection with *P. berghei* ANKA in Hb^{wt} mice was associated with the development of interstitial pneumonia and RBC extravasation as well as iron deposits, prominent in the liver. The latter can also be seen in *P. berghei* ANKA infected Hb^{SAD} mice, albeit to a lesser extent. Lungs of *P. berghei* ANKA infected Hb^{SAD} were only mildly affected, as compared to those of Hb^{wt} mice. The protective effect of Hb^{SAD} was lost in $Hb^{SAD}Hmox1^{+/-}$ and $Hb^{SAD}Nrf2^{+/-}$ mice. That is, $Hb^{SAD}Hmox1^{+/-}$ and and $Hb^{SAD}Nrf2^{+/-}$ showed massive pneumonia as well as iron deposits in the liver when infected with *P. berghei* ANKA.

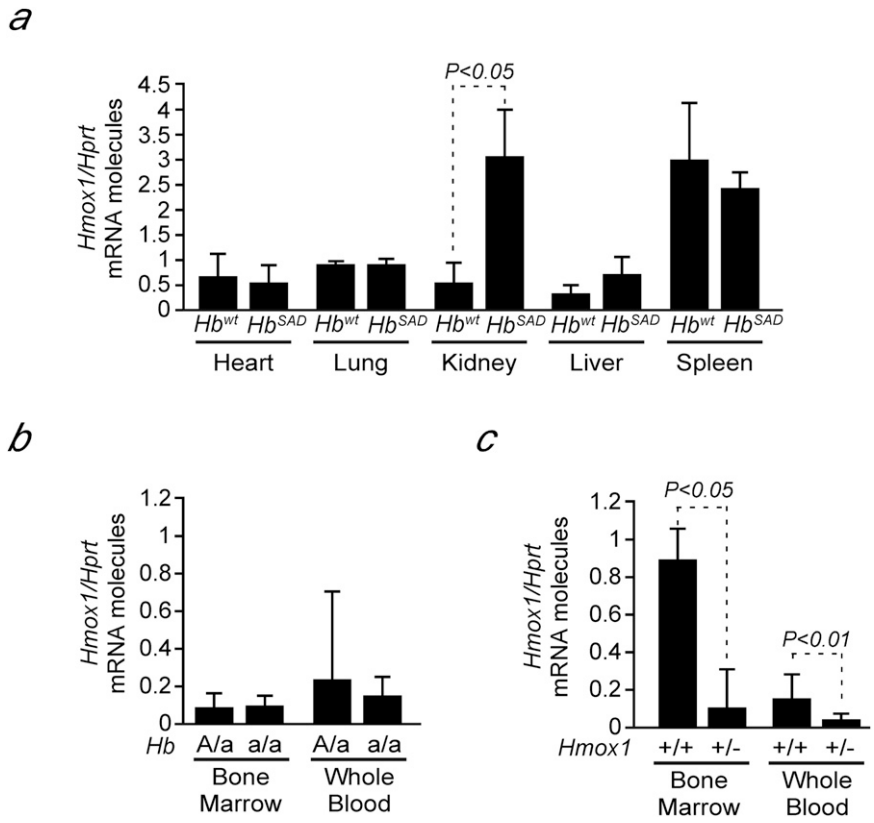

Figure S3. Modulation of HO-1 Expression in Different Experimental Settings, Related to Figure 2

Mean ratio of *Hmox1* versus hypoxanthine-guanine phosphoribosyltransferase (*Hprt*) mRNA molecules in ***a)*** different organs of naïve Hb^{wt} and Hb^{SAD} mice ± standard deviation (n=4/group), ***b)*** bone marrow and peripheral blood leukocytes of naïve $Hb^{A/a}$ and $Hb^{a/a}$ mice ± standard deviation (n=4) and ***c)*** bone marrow and peripheral blood leukocytes of naïve $Hb^{SAD}Hmox1^{+/+}$ and $Hb^{SAD}Hmox1^{+/-}$ mice ± standard deviation (n=4). Notice in (*b*) the lack of up-regulation of *Hmox1* mRNA expression in $Hb^{A/a}$ versus $Hb^{a/a}$ mice. Notice in (*c*) the significant decrease in the levels of *Hmox1* mRNA expression in Hb^{SAD} mice with only one ($Hmox1^{+/-}$) versus two ($Hmox1^{+/+}$) functional *Hmox1* alleles.

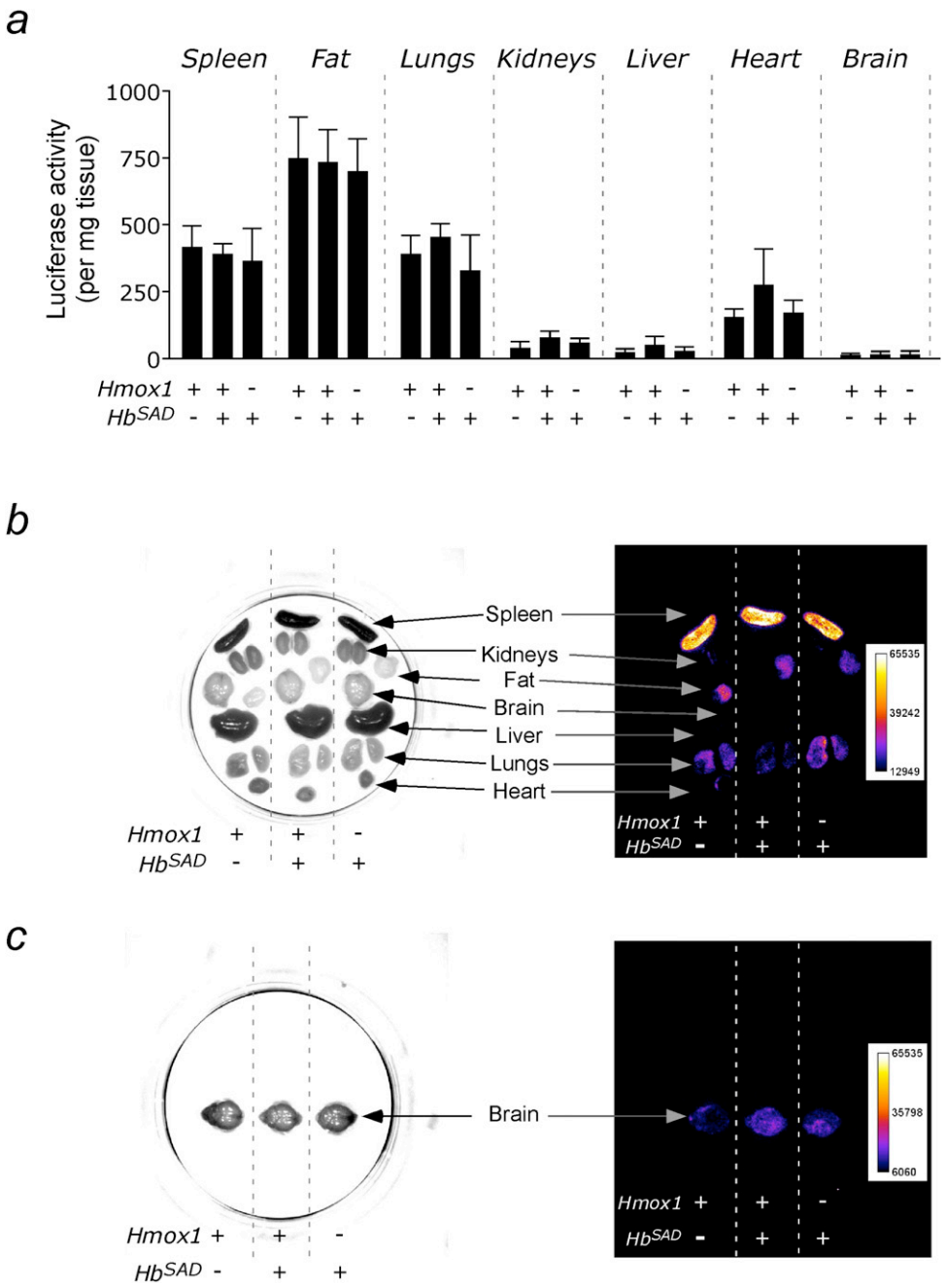

Figure S4. Neither Hb^{SAD} or HO-1 Regulate Plasmodium Sequestration, Related to Figure 2

(a) Mean ratio of Luciferase activity in different organs from $Hb^{wt}Hmox1^{+/+}$, $Hb^{SAD}Hmox1^{+/+}$ and $Hb^{SAD}Hmox1^{+/-}$ mice ± standard deviation (n=9/group), at day 7 postinfection with Luciferase-transgenic *P. berghei* ANKA. Pooled from 3 independent experiments with similar results (exposure time 15 sec).

(b) Visualization of Luciferase-transgenic *P. berghei* ANKA sequestration in the same mice as in (a) (exposure time 15 sec).

(c) Visualization of Luciferase-transgenic P. berghei ANKA sequestration in the brains of the same mice as in (a) (exposure time 2 min.).

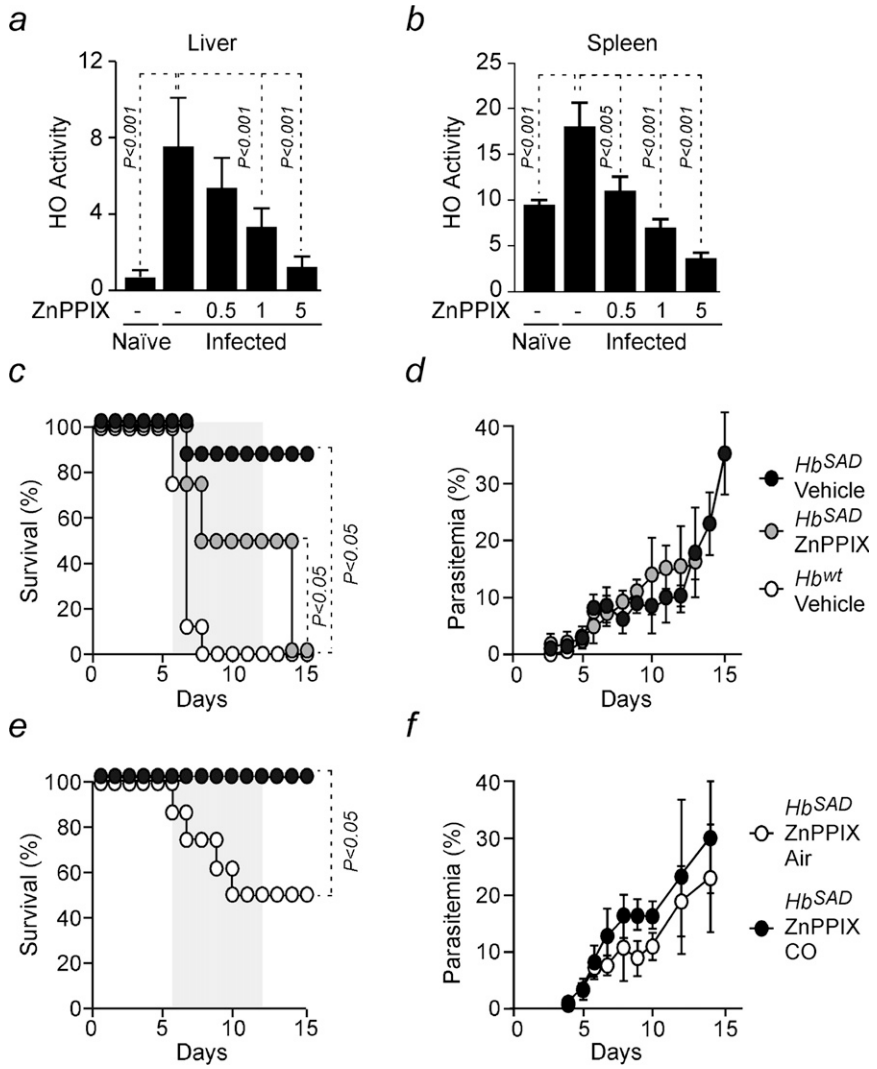

Figure S5. Pharmacologic inhibition of HO Activity Negates the Protective Effect of Sickle Hb against ECM, Related to Figure 2

HO activity was measured in ***a)*** liver and ***b)*** spleen of naïve or *P. berghei* ANKA infected Hb^{wt} mice receiving the HO enzymatic inhibitor ZnPPIX (mg/kg bw, every 12 hours from day 2 pre-infection to day 7 postinfection) or vehicle (-). Results are shown as mean percentage of HO enzymatic activity (pmol bilirubin/mg protein/h) ± standard deviation (n=5 mice/group). **c**) Survival of *P. berghei* ANKA-infected Hb^{SAD} mice receiving vehicle (n=8) or ZnPPIX (5mg/kg bw) as in (a) and (b)(n=8). Vehicle-treated *P. berghei* ANKA-infected Hb^{wt} mice were used as controls (n=8). Results shown were pooled from 2 independent experiments with similar results. ***d***) Mean percentage of infected RBC (parasitemia) in infected Hb^{SAD} mice receiving vehicle (n=8) or ZnPPIX (n=8) and in vehicle-treated Hb^{wt} mice (n=8) ± standard deviation. ***e***) Survival of *P. berghei* ANKA-infected Hb^{SAD} mice receiving ZnPPIX as in (a) and (b) and exposed to air (n=8) or CO (250 ppm, 4-7 days postinfection)(n=8). Results shown were pooled from 2 independent experiments with similar results. ***f***) Mean percentage of infected RBC (parasitemia) in the same mice as (e). Grey shadings in panels *(c)* and *(e)* indicate the expected time of ECM.

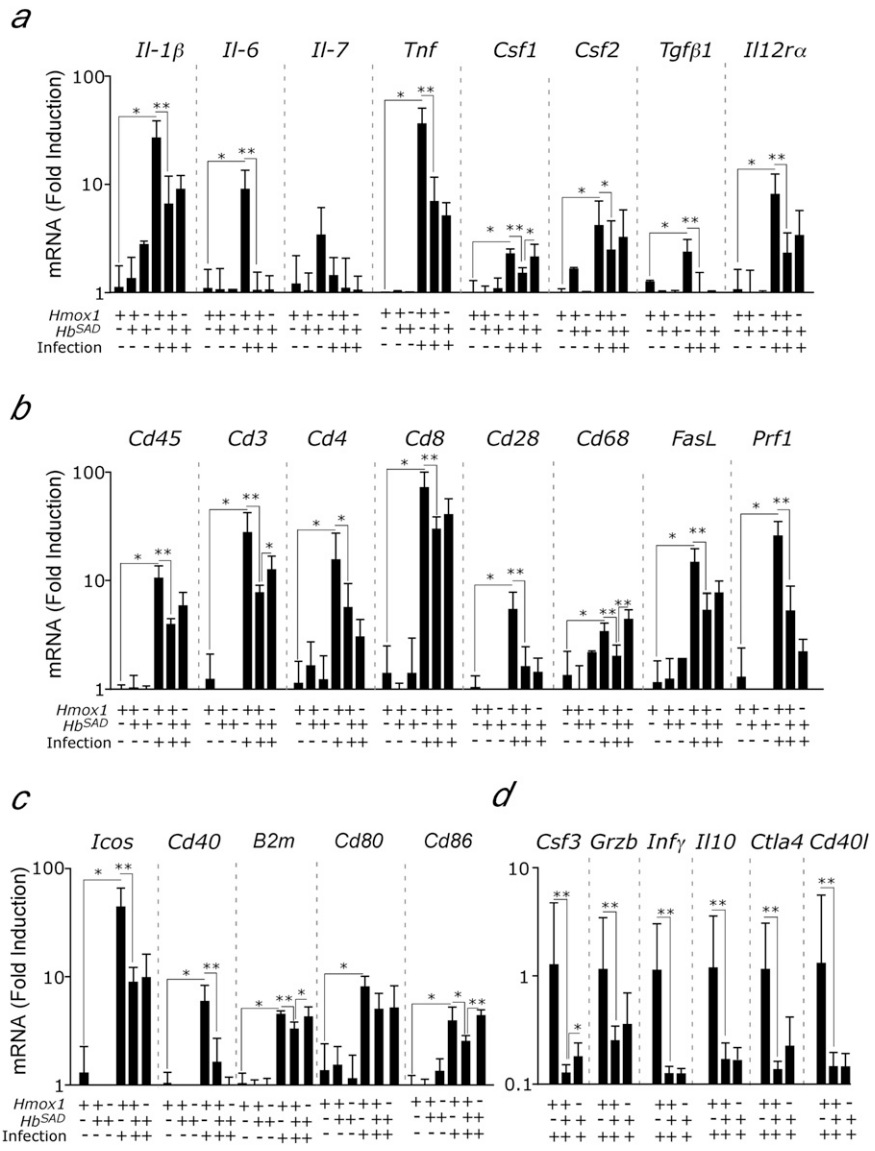

Figure S6. Hb^{SAD} Inhibits Neuroinflammation, Related to Figure 3

Quantification of mRNA encoding (***a***) cytokines, (***b***) molecules expressed by leukocyte, (***c***) co-stimulatory molecules expressed by antigen presenting cells and (***d***) diverse set of molecules, in the brains of naïve (-) versus *berghei* ANKA-infected infected (+) mice carrying one (-) or two (+) functional *Hmox1* alleles and expressing (+) *Hb^{SAD}* or not (-). Results are shown as mean ± standard deviation (n=4-8/group), analyzed at the time of ECM onset. Notice that inhibition of pro-inflammatory gene expression in *P. berghei* ANKA-infected *Hb^{SAD}* versus *Hb^{wt}* mice is similar whether the *Hb^{SAD}* mice have one (-) or two (+) functional *Hmox1* alleles. This suggests that *Hb^{SAD}* can exert protective effects independently of HO-1.

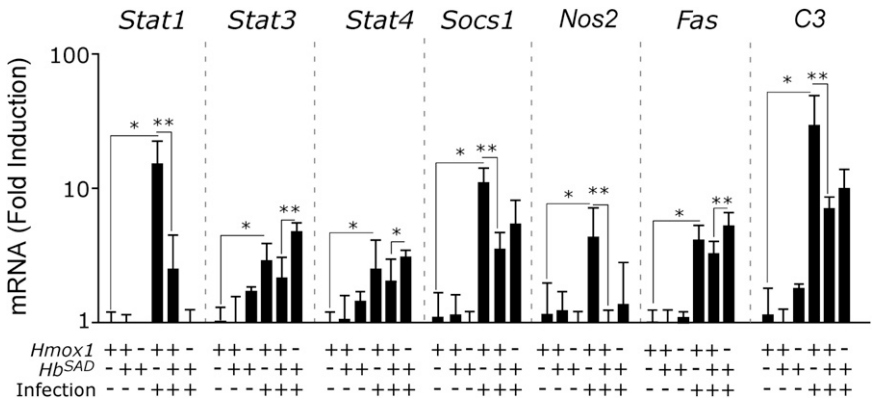

Figure S7. Hb^{SAD} Inhibits Neuroinflammation (Continued), Related to *Figure 3*

Quantification of mRNA encoding a diverse set of molecules, in the brains of naïve (-) versus *berghei* ANKA-infected infected (+) mice carrying one (-) or two (+) functional *Hmox1* alleles and expressing (+) Hb^{SAD} or not (-). Results are shown as mean ± standard deviation (n=4-8/group), analyzed at the time of ECM onset. Notice that inhibition of pro-inflammatory gene expression in *P. berghei* ANKA-infected Hb^{SAD} versus Hb^{wt} mice is similar whether the Hb^{SAD} mice have one (-) or two (+) functional *Hmox1* alleles, suggesting that Hb^{SAD} can exert protective effects independently of HO-1.

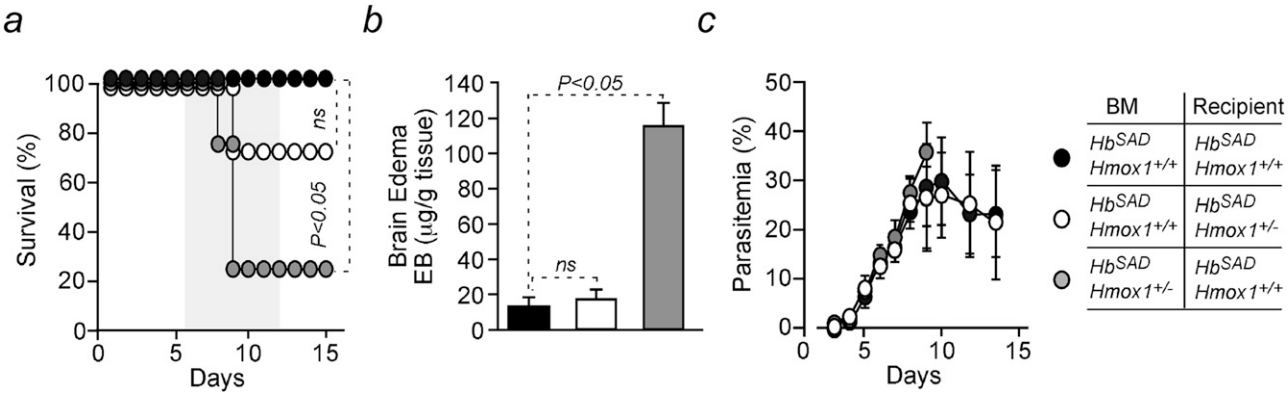

Figure S8. The Protective Effect of Sickle Hb against ECM Requires the Expression of HO-1 in Hematopoietic Cells, Related to *Figure 4*

(a) Survival of P. berghei ANKA-infected chimeric Hb^{SAD} mice resulting from the adoptive transfer of bone marrows from $Hb^{SAD}Hmox1^{+/+}$ mice into $Hb^{SAD}Hmox1^{+/+}$ recipients (n=6); from $Hb^{SAD}Hmox1^{+/+}$ mice into $Hb^{SAD}Hmox1^{+/-}$ recipients (n=7) and from $Hb^{SAD}Hmox1^{+/-}$ mice into $Hb^{SAD}Hmox1^{+/+}$ recipients (n=8). Recipients were lethally irradiated before the adoptive transfer. Grey shading indicates expected time of ECM. Results shown were pooled from 5 independent experiments.

(b) Brain edema was measured by Evans blue (EB) accumulation in brains of chimeric mice, produced as in (*a*). Results are shown as mean ± standard deviation (n=3/group).

(c) Mean percentage of infected RBC in chimeric mice, produced as in (*a*). Results are shown as mean ± standard deviation. Same mice as in (a).

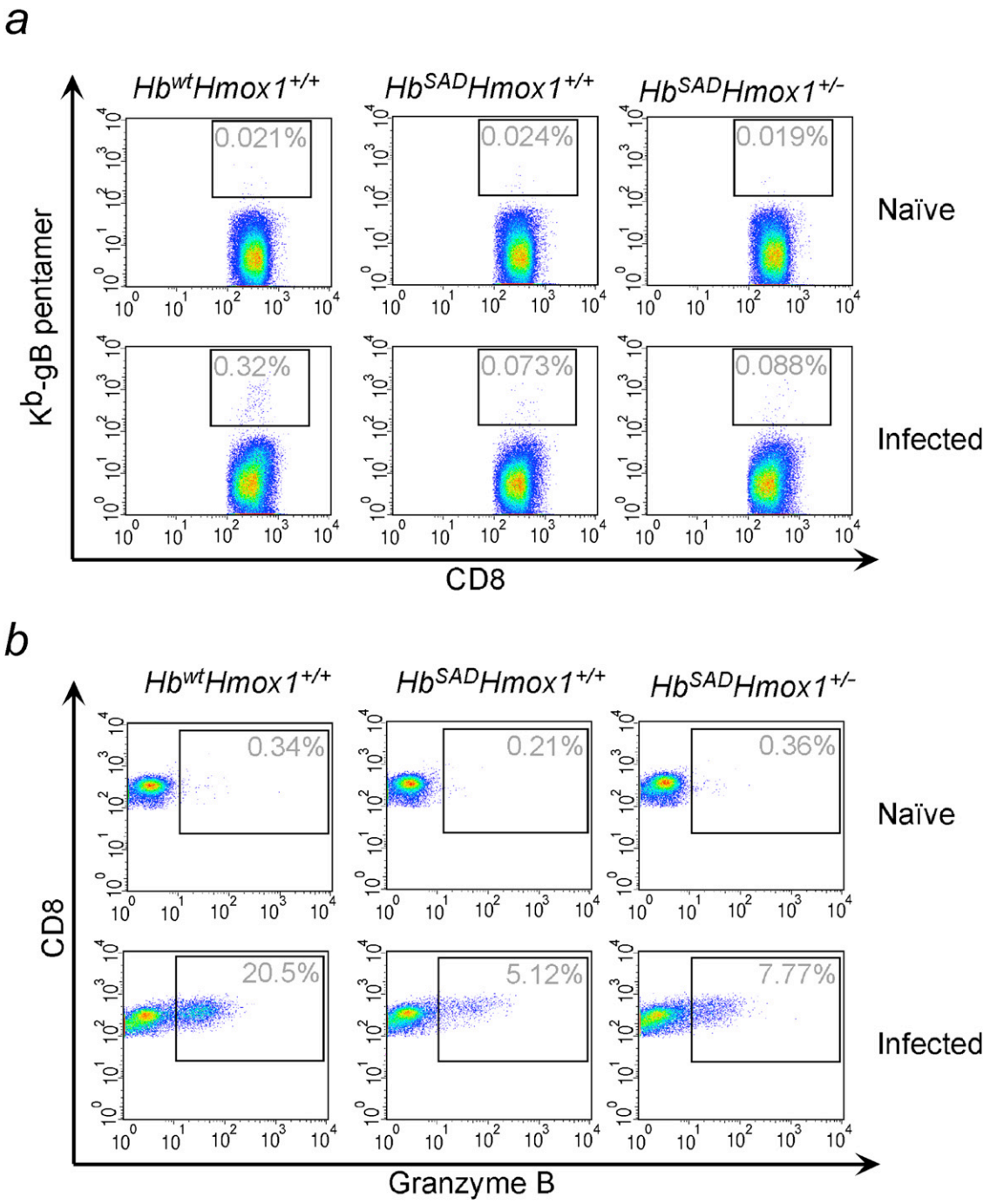

Figure S9. The Immunoregulatory Effect of Hb^{SAD} Does Not Involve HO-1, Related to Figure 4

Representative flow cytometry dot plots of ***a)*** $CD8^+$ T cells specific for the *P. berghei* ANKA encoded MHC I-restricted epitope derived from glycoprotein B of herpes simplex virus-1 ($gB_{498-505}$) and ***b)*** $CD8^+GrB^+$ T cells, in the spleen of $Hb^{wt}Hmox1^{+/+}$, $Hb^{SAD}Hmox1^{+/+}$ and $Hb^{SAD}Hmox1^{+/+}$ mice not infected or 5 days after *P. berghei* ANKA infection. Numbers in gray indicate the percentage of cells inside the gates.

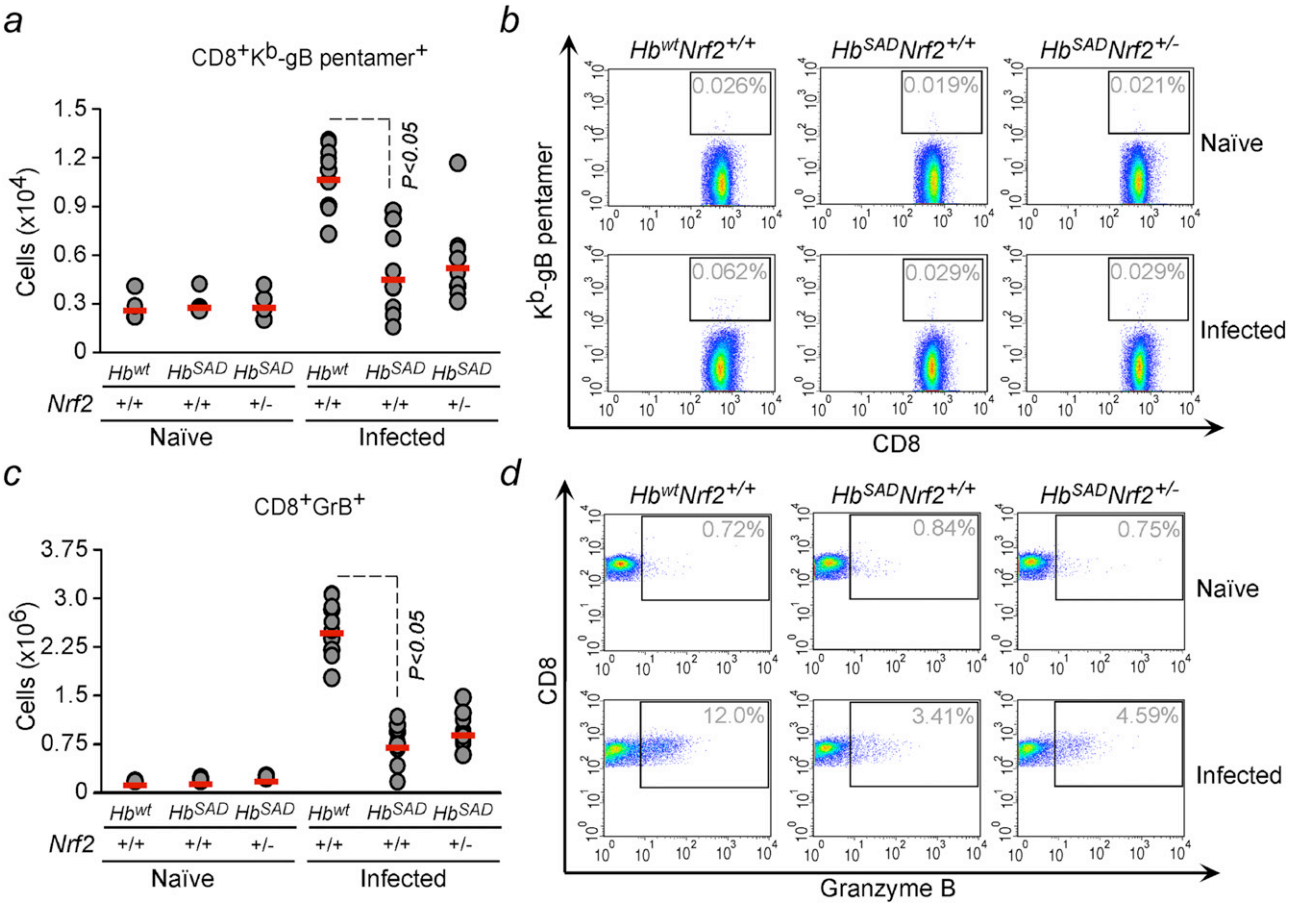

Figure S10. The Immunoregulatory Effect of Hb^{SAD} Does Not Involve the Transcription Factor Nrf2, Related to Figure 5

(a) Number of CD8$^+$ T cells specific for the *P. berghei* ANKA encoded MHC I-restricted epitope derived from glycoprotein B of herpes simplex virus-1 (gB$_{498\text{-}505}$), in the spleen of *Hb^{wt}Nrf2$^{+/+}$*, *Hb^{SAD}Nrf2$^{+/+}$* and *Hb^{SAD}Nrf2$^{+/-}$* mice not-infected (naïve) or 5 days after *P. berghei* ANKA infection.

(b) Representative flow cytometry dot plots of splenic CD8$^+$ T cells recognizing the gB$_{498\text{-}505}$ epitope in the same mice as in (a).

(c) Number of splenic CD8$^+$GrB$^+$ T cells in the same mice as in (a).

(d) Representative flow cytometry dot plots of splenic CD8$^+$GrB$^+$ T cells in the same mice as in (c). Circles in (a) and (c) represent single mice and red lines mean values (n=4 and n=10 in noninfected and infected groups, respectively), pooled from 2 independent experiments with similar results. Numbers in gray (b) and (d) indicate the percentage of cells inside the gates.

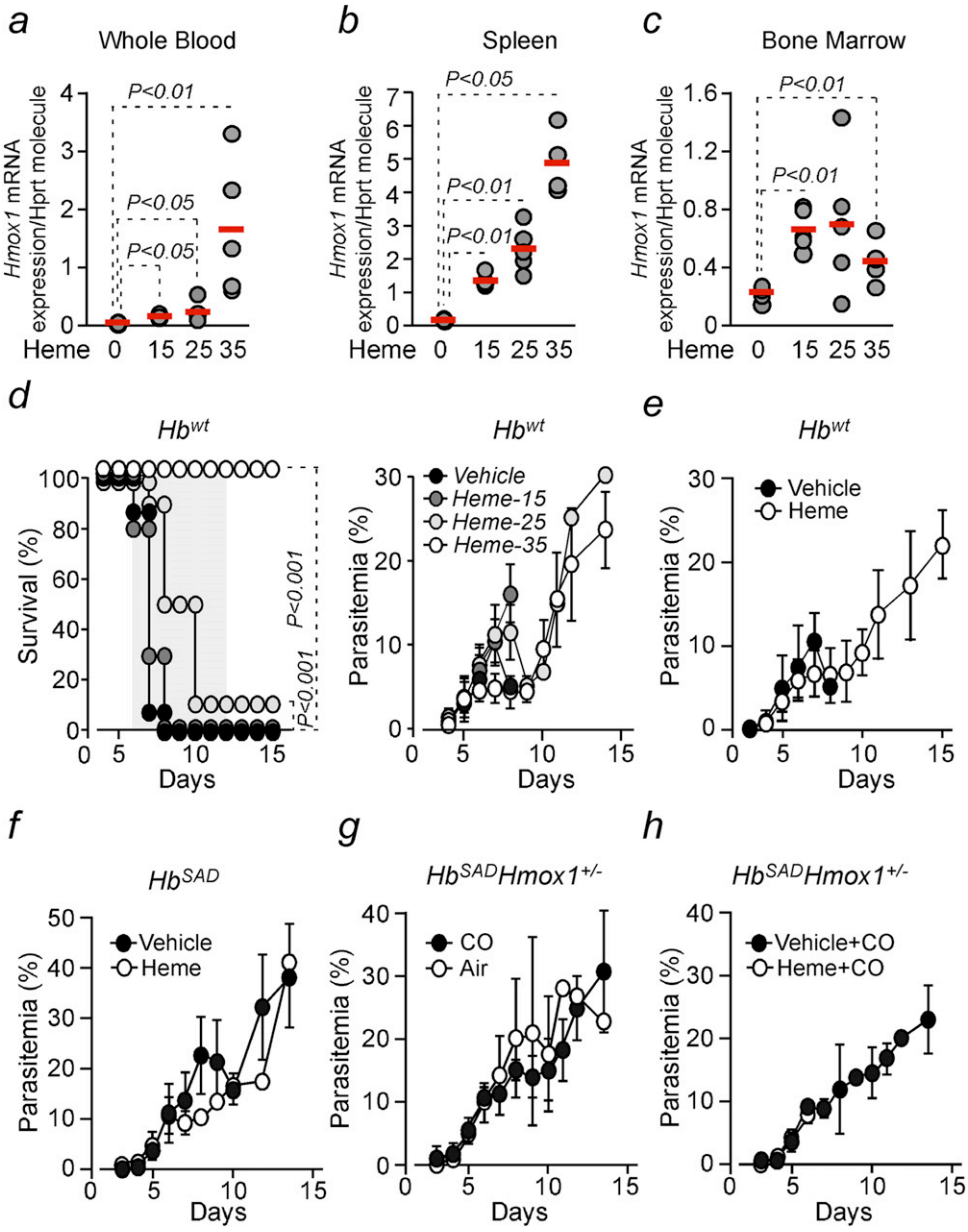

Figure S11. Heme Regulates HO-1 Expression and Confers Tolerance to Plasmodium Infection via CO, Related to Figure 6

Hmox1 mRNA was measured by qRT-PCR in the ***a)*** whole blood ***b)*** spleen and ***c)*** bone marrow of Hb^{wt} mice 12 hours after receiving heme at the dosage indicated (mg/kg bw; i.p.). Circles represent single mice and red lines mean values (n=4-5/group), ***d***) Survival and mean percentage ± standard deviation of *P. berghei* ANKA-infected RBC (parasitemia) in Hb^{wt} mice receiving vehicle (n=15) or heme (mg/kg bw, every 48h, from day 2 pre-infection to 4 postinfection; n=9-10/group). Results shown were pooled from three independent experiments, with similar results. ***e)*** Mean percentage of *P. berghei* ANKA-infected RBC (parasitemia) in infected Hb^{wt} mice receiving vehicle (n=25) or heme (35-40 mg/kg bw, every second day; from day 2 pre-infection to day 7 postinfection; n=17) ± standard deviation. ***f)*** Mean percentage of infected RBC (parasitemia) in Hb^{SAD} mice receiving vehicle (n=8) or heme (days 4-7 postinfection, 30 mg/kg bw, every 12 h; n=8) ± standard deviation. ***g)*** Mean percentage of *P. berghei* ANKA-infected RBC (parasitemia) in infected $Hb^{SAD}Hmox1^{+/-}$ mice exposed to air (n=8) or CO (250 ppm, days 4-7 postinfection; n=12) ± standard deviation. ***h)*** Mean percentage of *P. berghei* ANKA-infected RBC (parasitemia) in infected $Hb^{SAD}Hmox1^{+/-}$ mice exposed to CO (250 ppm, days 4-7 postinfection) and receiving vehicle or heme (days 4-7 postinfection, 25 mg/kg bw, every 12 h; n=8) ± standard deviation.

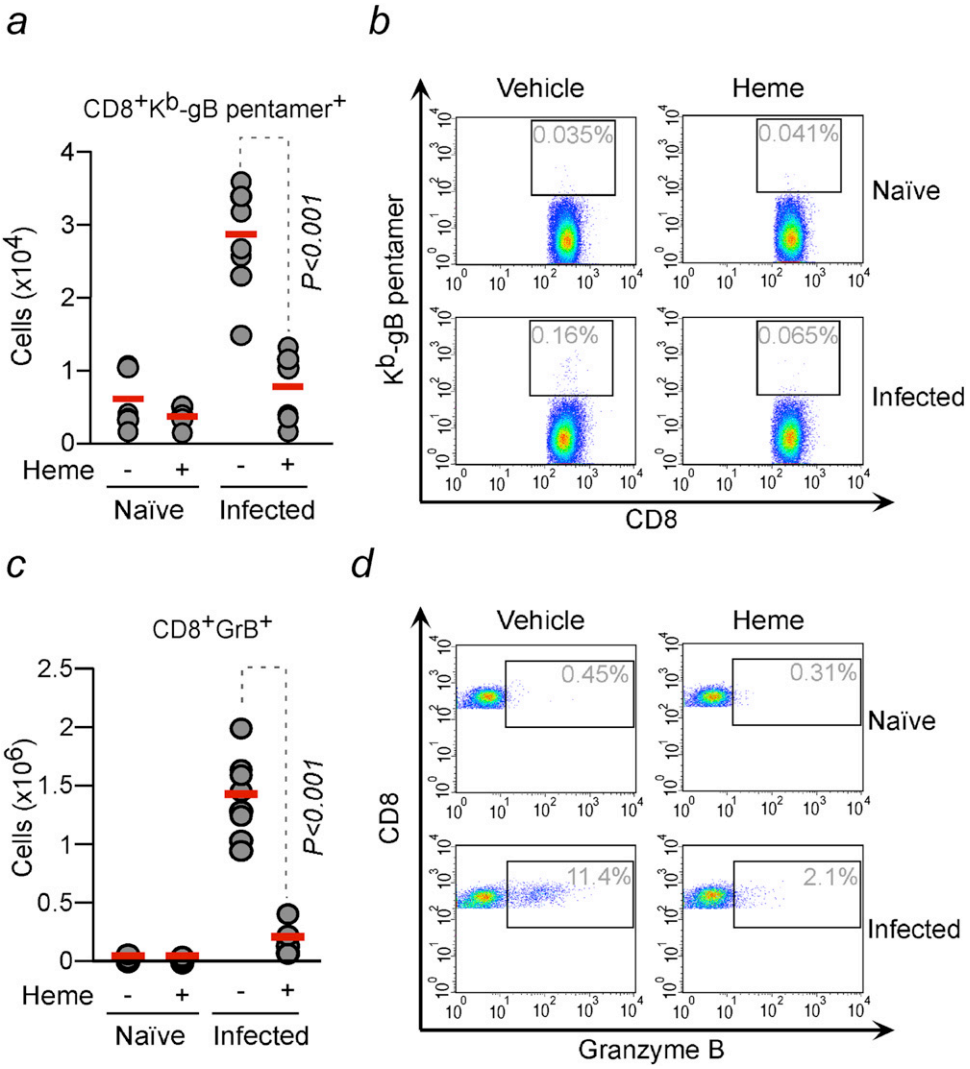

Figure S12. Heme Administration before Plasmodium Infection Mimics the Immunoregulatory Effect of Hb^{SAD}, Related to Figure 6

(***a***) Number of $CD8^+$ T cells specific for the *P. berghei* ANKA encoded MHC I-restricted epitope derived from glycoprotein B of herpes simplex virus-1 ($gB_{498-505}$), in the spleen of Hb^{wt} mice infected or not (naïve) with *P. berghei* ANKA (5 days postinfection). Hb^{wt} received (+) or not (-) heme (35 mg/kg, i.p., every 48h, from day 2 pre-infection to 4 postinfection).

(***b***) Representative flow cytometry dot plots of splenic $CD8^+$ T cells recognizing the $gB_{498-505}$ epitope in the same mice as in (a).

(***c***) Number of splenic $CD8^+GrB^+$ T cells in the same mice as in (a). (d) Representative flow cytometry dot plots of splenic $CD8^+GrB^+$ T cells in the same mice as in (c). Circles in (a) and (c) represent single mice and red lines mean values (n=6-8/group), pooled from 2 independent experiments with similar results. Numbers in gray (b and d) indicate the percentage of cells inside the gates.